Various structures of the neutron-rich nucleus ^{31}Mg investigated by β–γ spectroscopy of spin-polarized ^{31}Na

Hiroki Nishibata

Nuclear Spectroscopy Laboratory, RIKEN

PhD work
at Osaka Univ.

- Applications of spin polarization to nuclear structure study.
- Unique method to assign spin-parity of excited levels based on β–γ spectroscopy of spin-polarized Na isotopes.
- Investigation of nuclear structure of their daughters, i.e., Mg isotopes.

Physics motivation

Deformed ground states of neutron rich nuclei with N~20

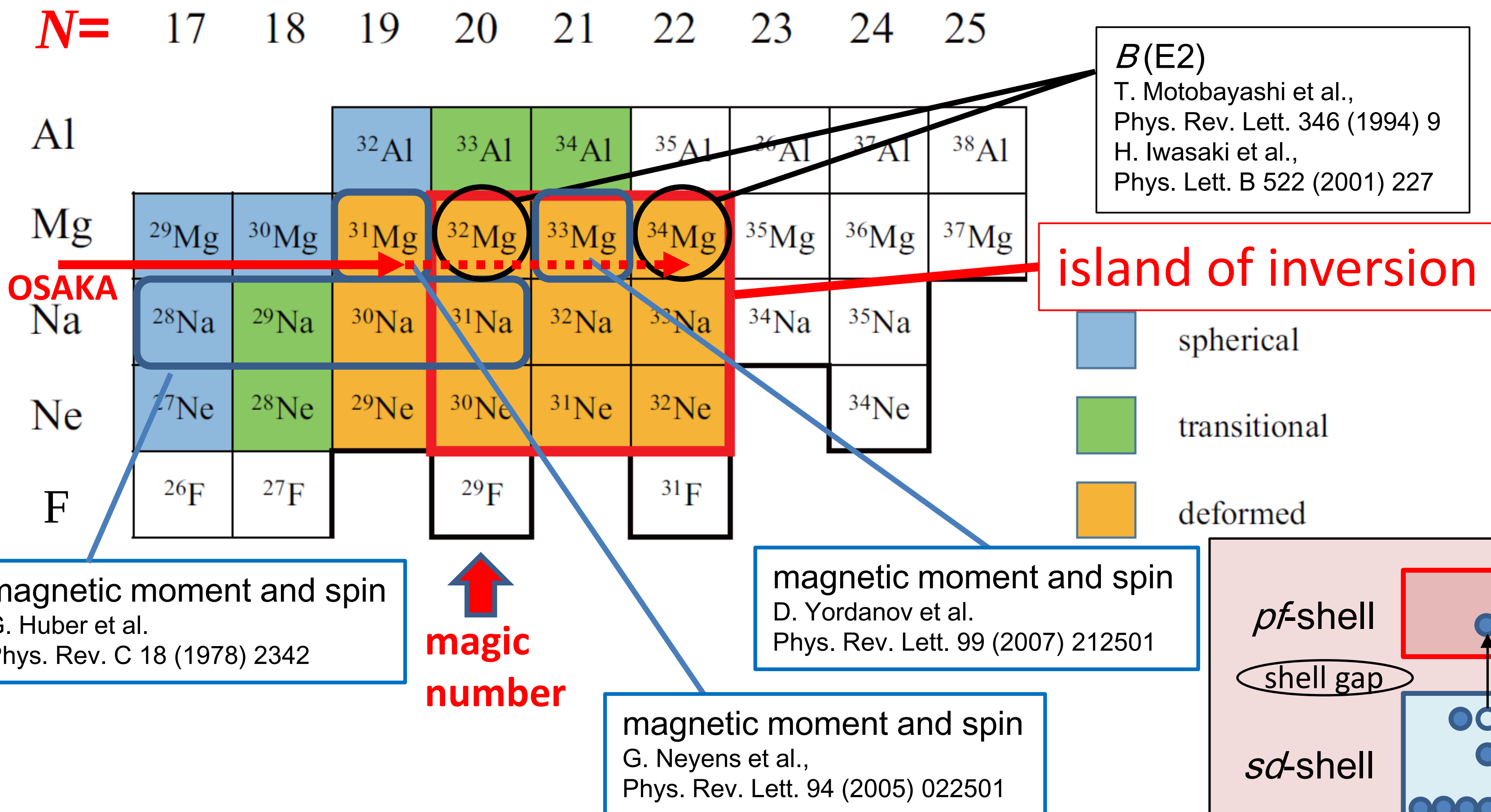

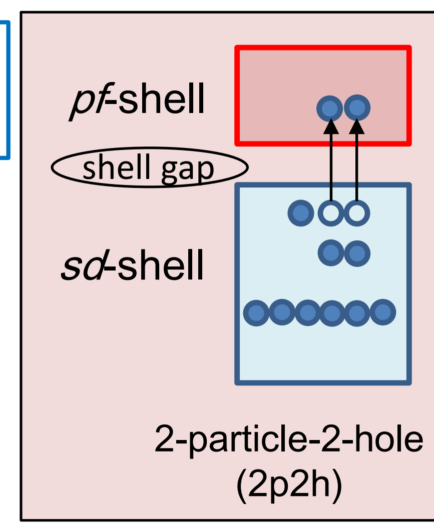

Many experimental and theoretical investigations have been performed since 1970's.

Large-scale Shell Model calculations

Caurier et al., Phys.Rev. C 90 (2014) 014302

SDPF-U-MIX interaction
model space **n: sd-pf**, p: sd

across the N=20 “shell gap”

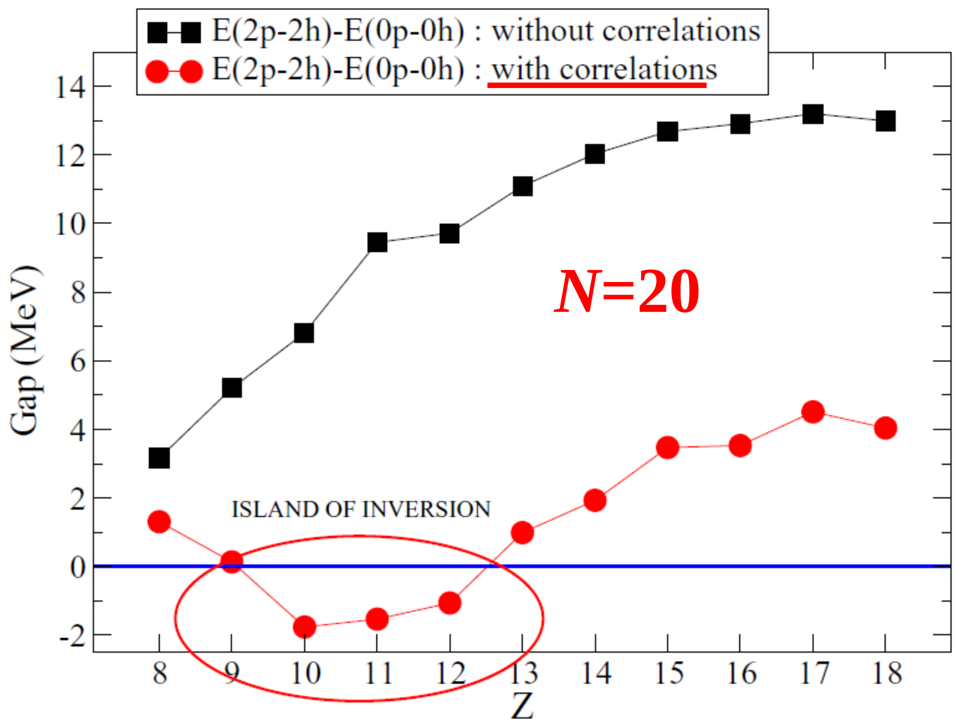

FIG. 5. (Color online) The gap between the 0p-0h and the 2p-2h configurations at $N = 20$, without correlations (squares) and including correlations (circles). Nuclei close to or below the zero line are candidates to belong to the island of inversion.

- Nuclear correlations pull down the (2p-2h) level energies, and in some cases they become **lower** than the normal (0p-0h) level energies.

- The existence of islands of inversion or deformation are explained as the result of the **competition** between

  (1) the spherical mean field

  and

  (2) nuclear correlations which favor the deformed configurations.

Shape coexistence

competition between spherical mean field and nuclear correlation which drives deformation

investigation of shape coexistence in the low excitation energy region

comparison of the experimental and theoretical levels on the level-by-level basis

Today's talk : ^{31}Mg (N=19)

Various structures in ^{31}Mg

predicted by anti-symmetrized molecular dynamics plus generator coordinate method (AMD+GCM)

With assuming neither deformation nor mean field, this theory predicts both collective structures and single-particle structures in low excitation energy region.

The 1/2+ ground state is successfully predicted.

shape coexistence in ^{31}Mg

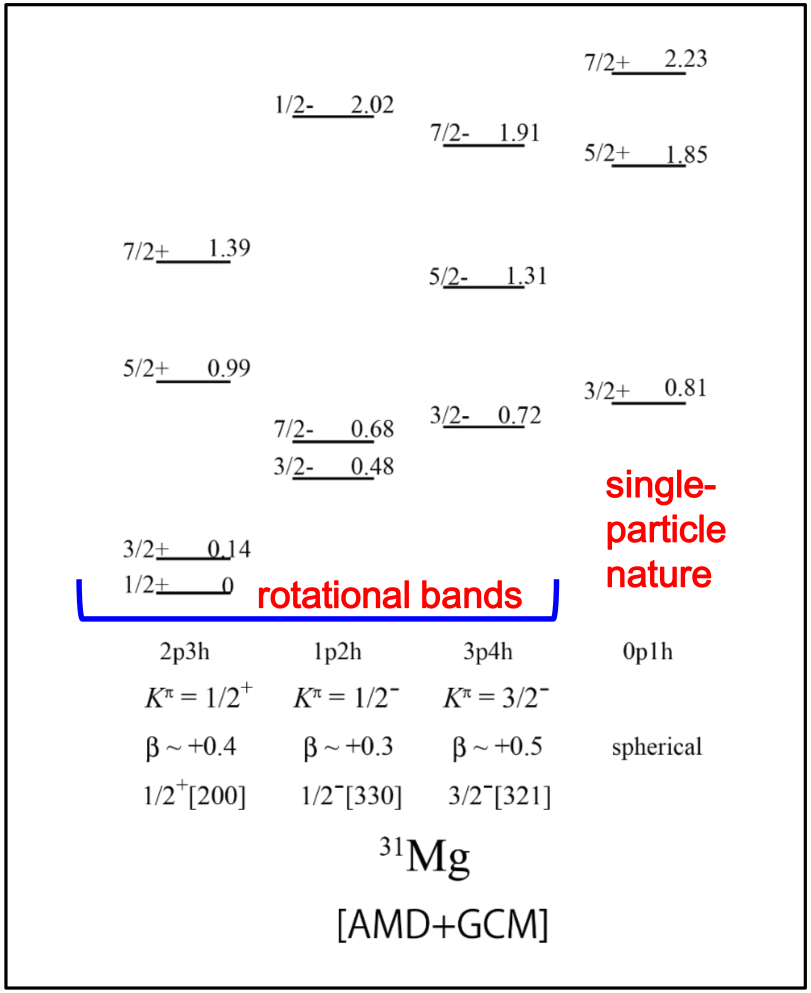

M. Kimura,
Phys. Rev. C 75(2007)041303(R)

Discovery history of ^{31}Mg levels

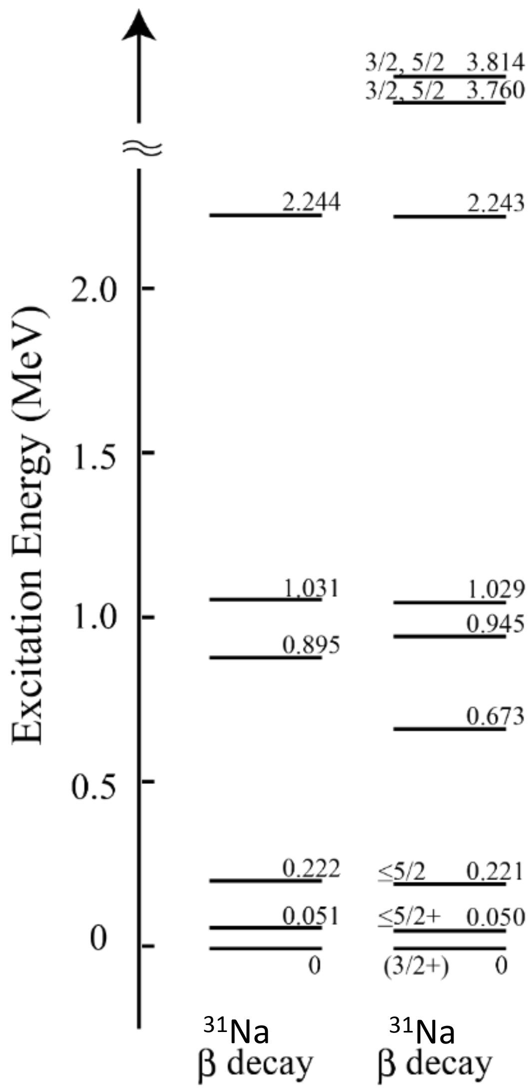

(year) **(1984)** (1993)

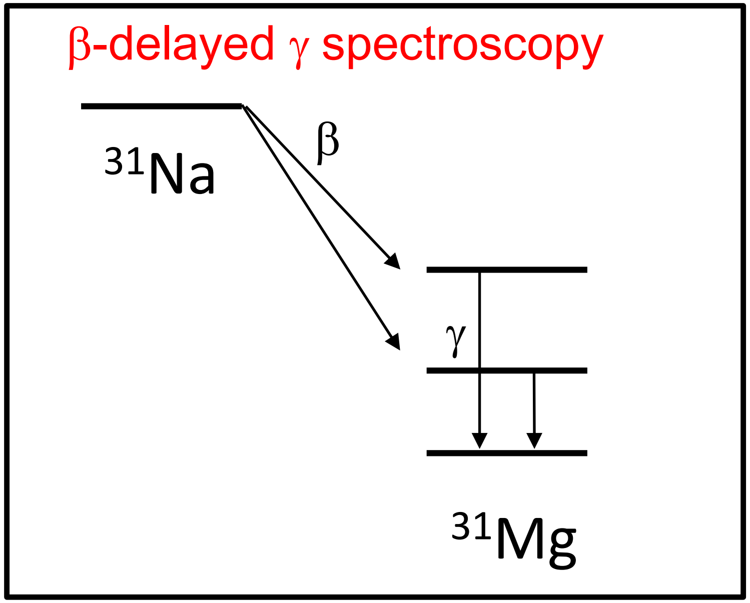

no spin-parity assignments

D. Guillemaud-Mueller et al., Nucl. Phys. A426 (1984) 37

G. Klotz et al., Phys. Rev. C 47 (1993) 2502

Discovery history of ^{31}Mg levels

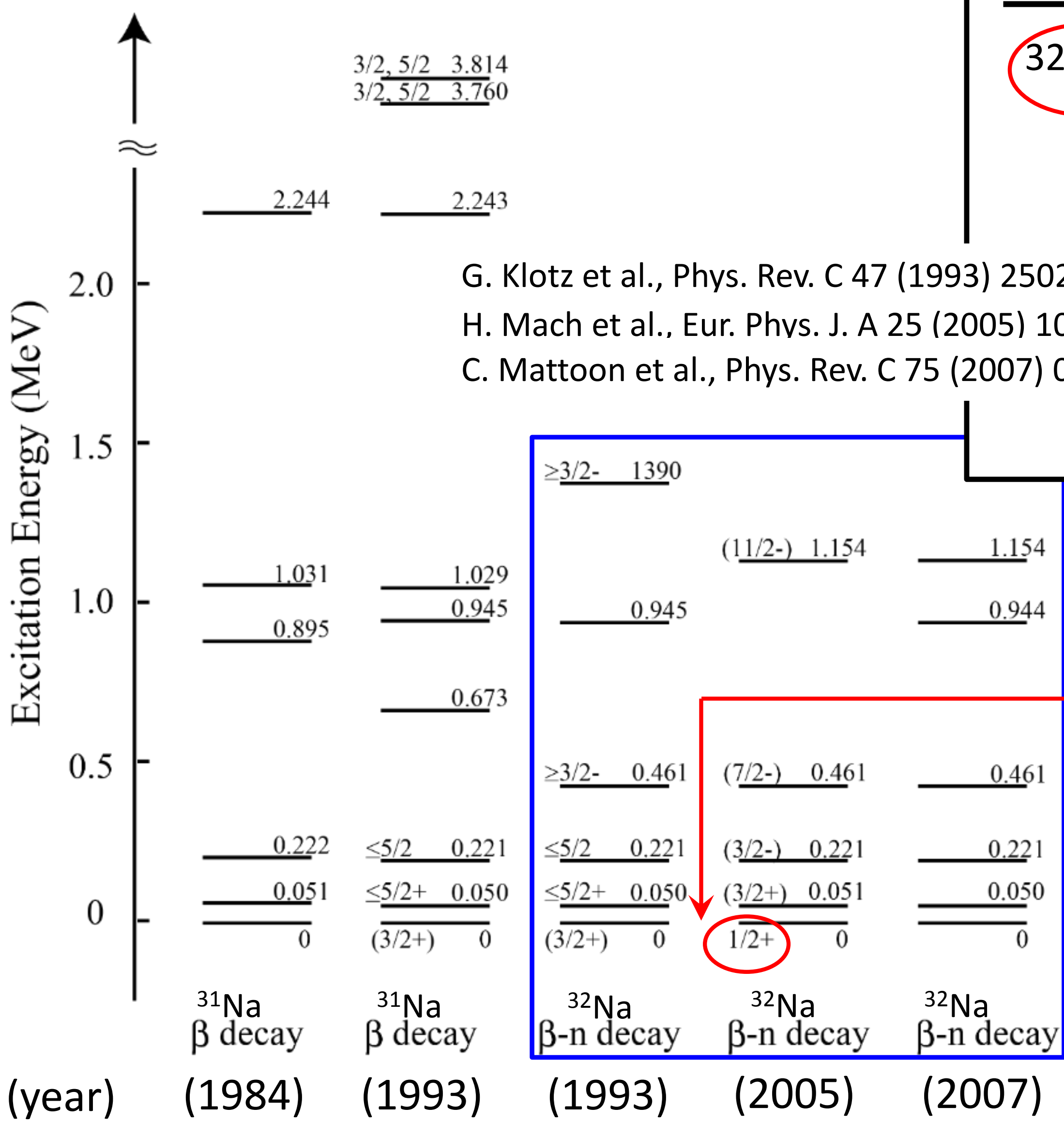

G. Klotz et al., Phys. Rev. C 47 (1993) 2502

H. Mach et al., Eur. Phys. J. A 25 (2005) 105

C. Mattoon et al., Phys. Rev. C 75 (2007) 017302

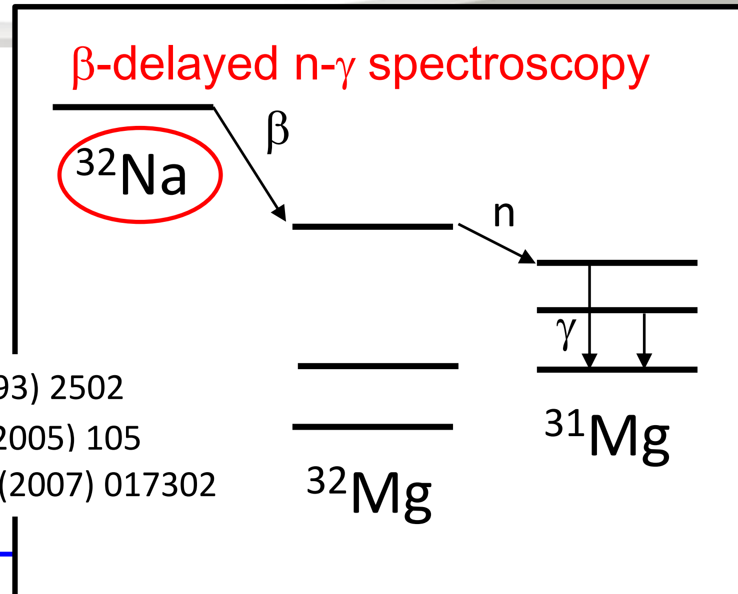

Unexpected spin-parity 1/2+ was determined in 2005 by combined measurements of hyperfine-structure and β – NMR.

G. Neyens et al,
Phys. Rev. Lett. 94 (2005) 022501

Discovery history of ^{31}Mg levels

- one-neutron-removal reaction from ^{32}Al
- one-proton-removal reaction from ^{32}Mg
- Coulomb excitation of ^{31}Mg

J. Terry et al., Phys. Rev. C 77 (2008) 014316
D. Miller et al., Phys. Rev. C 79 (2009) 054306
Seidlitz et al., Phys. Lett. B 700 (2011) 181

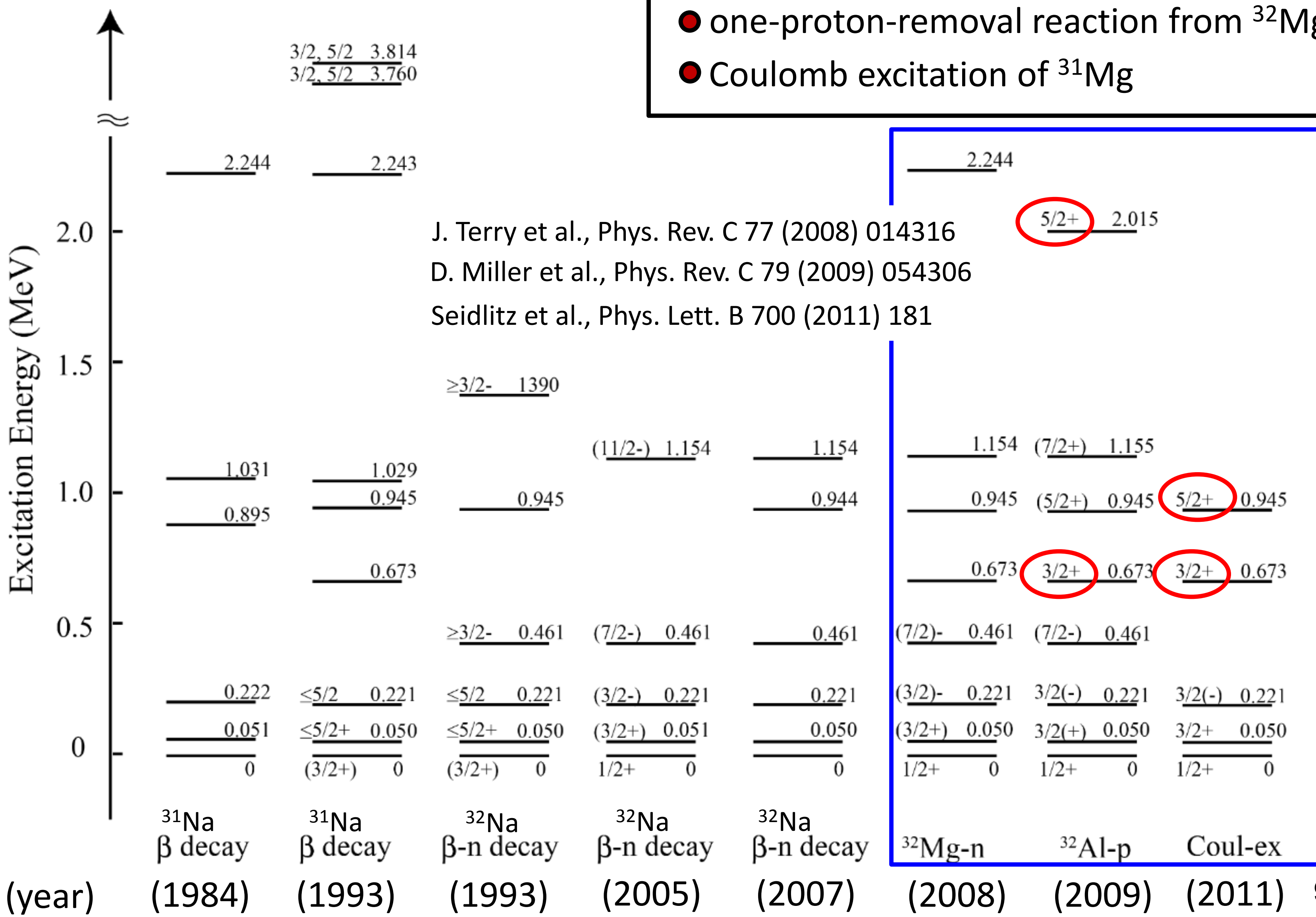

Adopted levels in ^{31}Mg by NNDC (updated in 2013)

Most of the spins and parities are unassigned, except for the 1/2+ ground state.

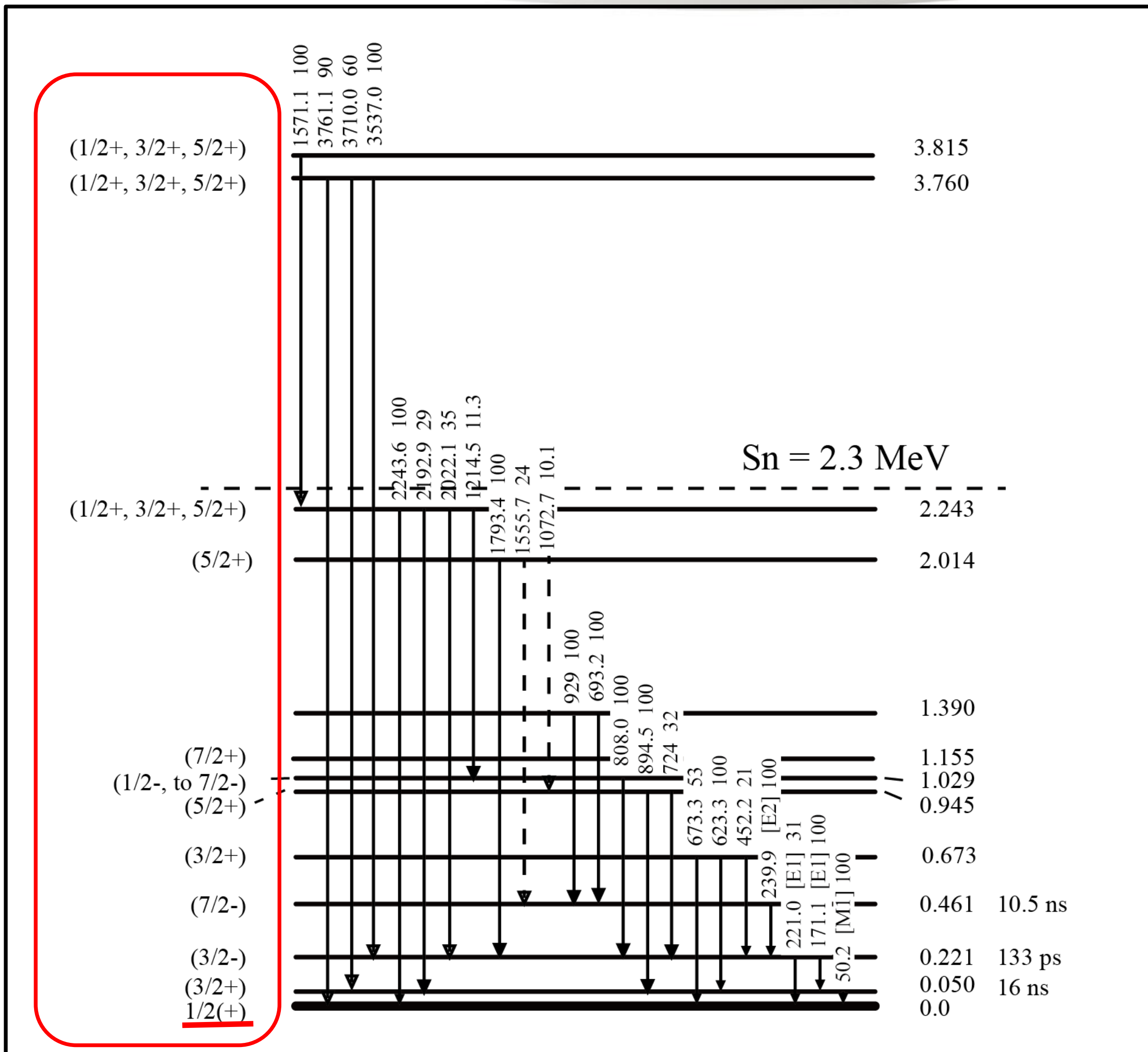

Firm spin-parity assignments are essential to understand the structure of ^{31}Mg.

Our method uses spin-polarized ^{31}Na to unambiguously assign the spins and parities of the levels in ^{31}Mg.

Principle of the measurement

and

Experiment

How to assign spin-parity of ^{31}Mg states

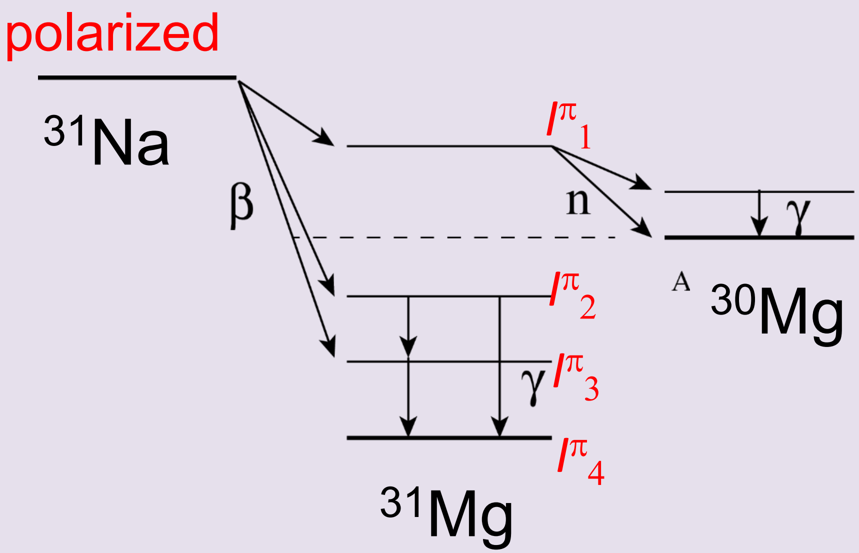

angular distribution of β-rays from polarized nucleus

allowed transition

$$W(\theta) \cong 1 + AP\cos\theta$$

A : asymmetry parameter of β-decay

P : spin polarization of parent nucleus

θ : emission angle of β-rays with respect to polarization axis

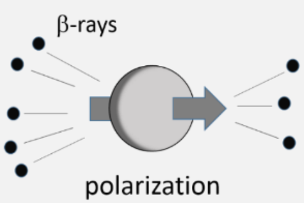

in the case

$A = -1,\ P = 0.5 \Rightarrow W(180^\circ) / W(0^\circ) = 3$

Asymmetry parameter *A*

The asymmetry parameter A is a constant depending on the daughter state spin value.

allowed transition

$$A(I_i, I_f) \begin{cases} = \dfrac{I_i}{I_i+1} & (\text{for} \quad I_f = I_i + 1) \\ \simeq \dfrac{-1}{I_i+1} & (\text{for} \quad I_f = I_i) \\ = -1 & (\text{for} \quad I_f = I_i - 1) \end{cases}$$

I_i: the parent spin
I_f: the daughter state spin

very discrete values

I_i^{π} (**^{31}Na**)	I_f^{π} (**^{31}Mg**)	A
3/2+	5/2+	+0.6
	3/2+	-0.4
	1/2+	-1.0

experimental A ⇒ spin of ^{31}Mg state

parity = + for allowed transitions

How to measure asymmetry parameter *A*

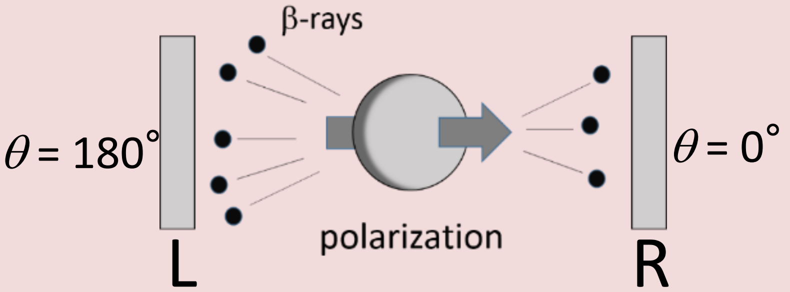

$$W(\theta) \cong 1 + AP\cos\theta$$

$$N_{R+} = N \times \varepsilon_R \times (1 + AP)$$

$$N_{L+} = N \times \varepsilon_L \times (1 - AP)$$

spin flip
every 100sec

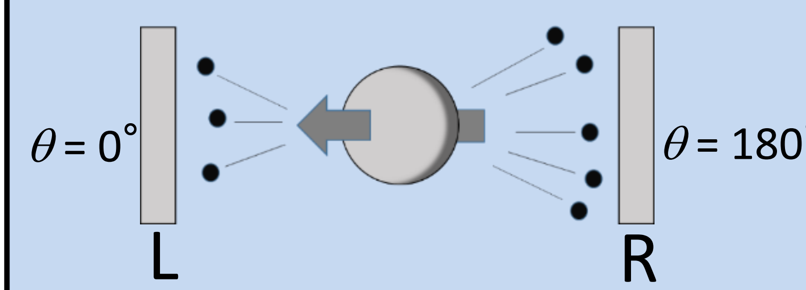

$$W(\theta) \cong 1 + AP\cos\theta$$

$$N_{R-} = N \times \varepsilon_R \times (1 - AP)$$

$$N_{L-} = N \times \varepsilon_L \times (1 + AP)$$

ε : efficiency *N* : Total β decay counts

AP-values are measured freely from instrumental asymmetry.

$$AP = \frac{\sqrt{R}-1}{\sqrt{R}+1} \quad \left(R = \frac{N_{L+}/N_{R+}}{N_{L-}/N_{R-}}\right)$$

P is common for all β-transitions
and can be determined by comparing two transitions.

Polarized ^{31}Na beam at TRIUMF in Canada

Target fragmentation:
500 MeV 10 μA proton beam
with UCx target

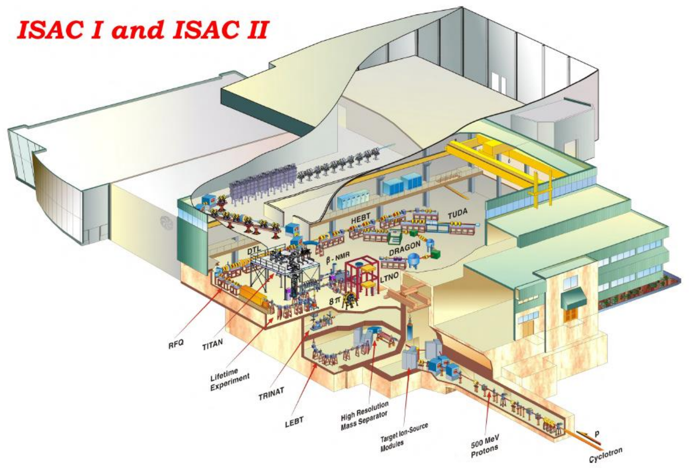

^{31}**Na+ ion beam intensity**:
~ 800 pps (extracted), 28keV
~ 200 pps (after polarizer)

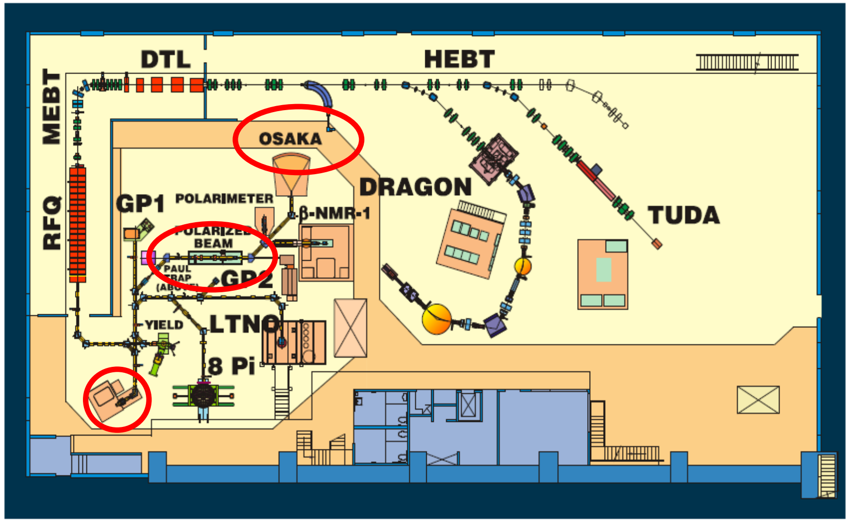

Polarizer at ISAC TRIUMF

spin polarization:
collinear laser optical pumping

P ~30%

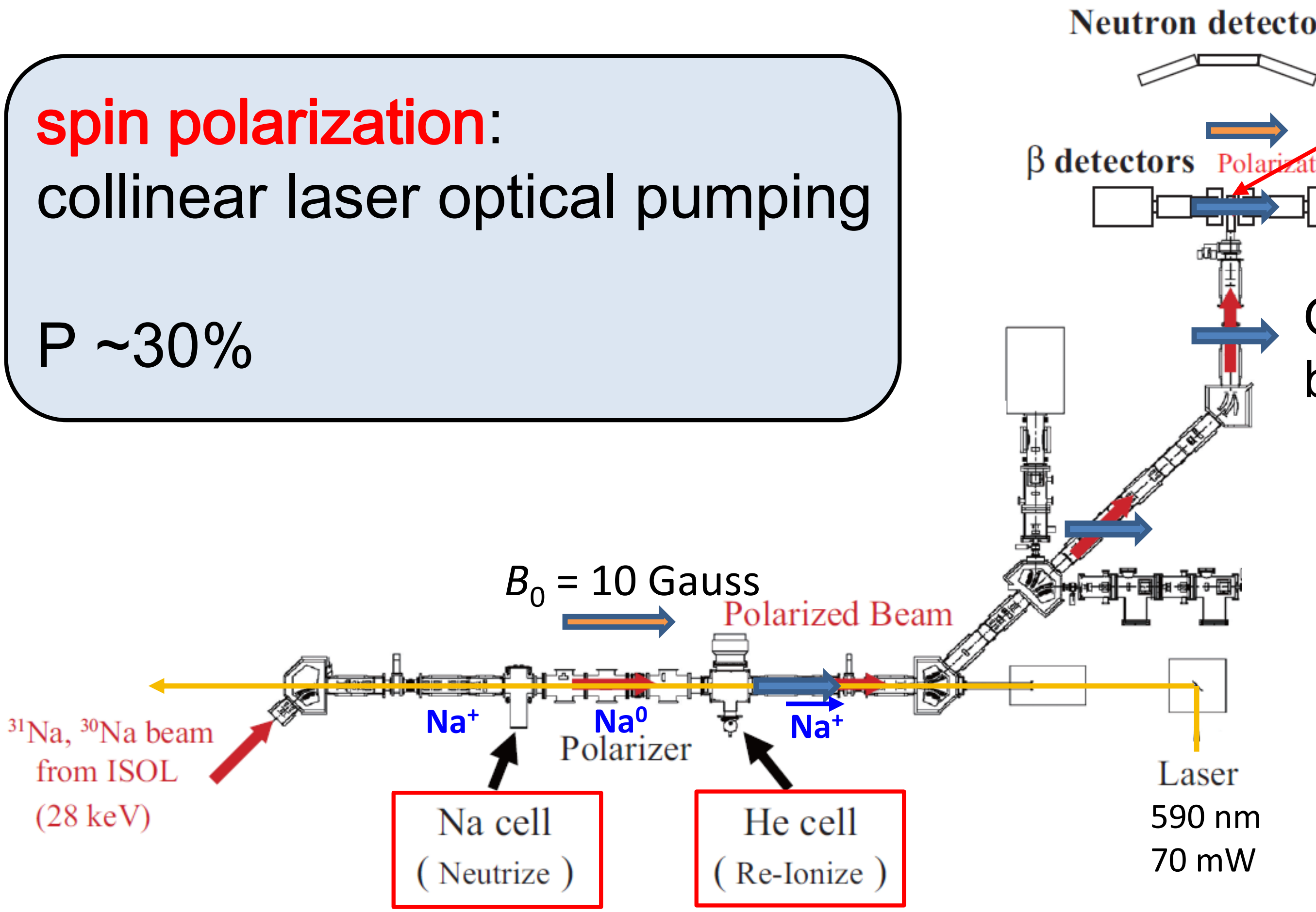

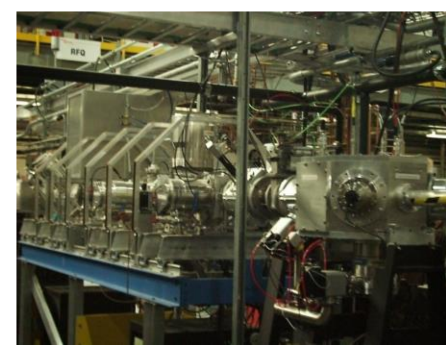

achieved effective pol.
***P* ~ 32%**

Detector Setup

β-asymmetry: β–γ, β–γ–γ, β–n
coincidence: γ–γ, n–γ

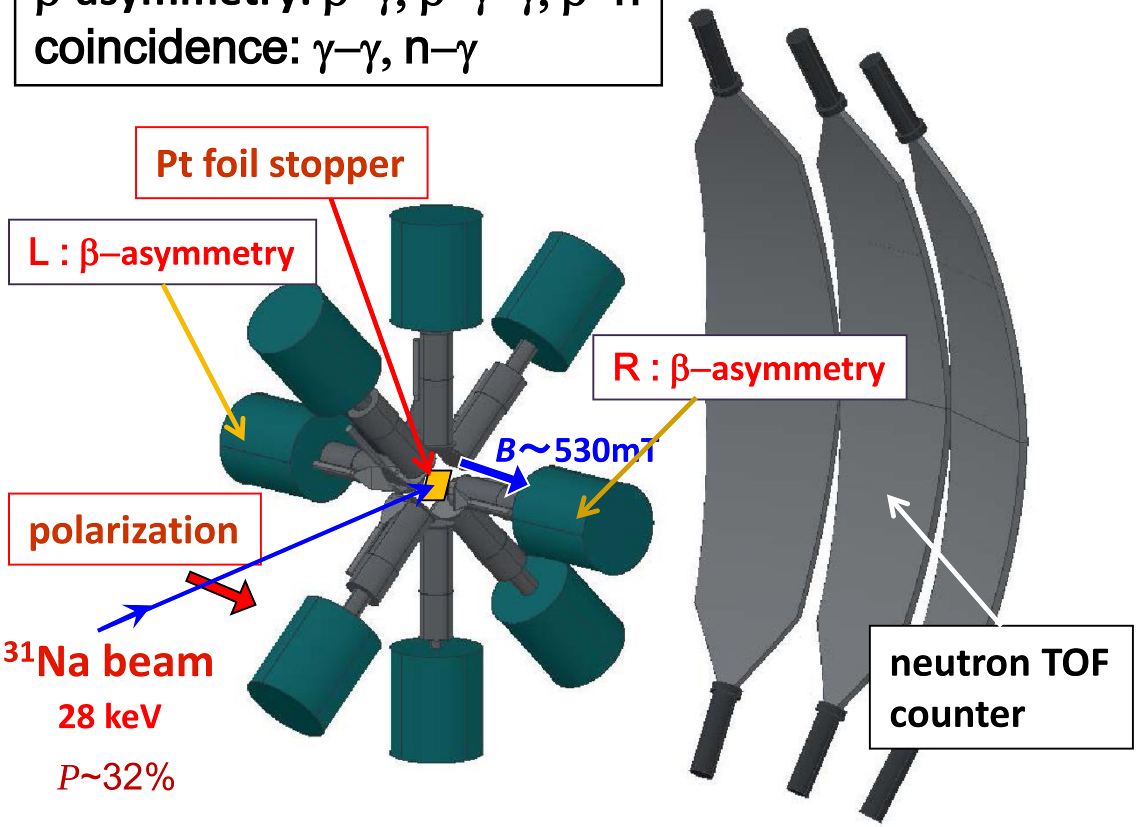

β, γ identification and β-ray energy measurement

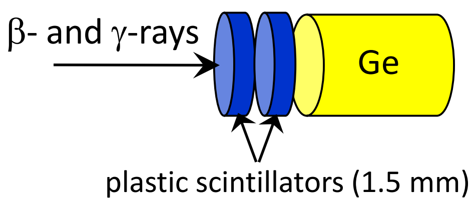

8 x (HPGe +2 plastic)
3 neutron TOF counters

β-detection efficiency: 15%
γ-detection efficiency: 2.9% @1333keV
n-detection efficiency: 0.2%@2MeV

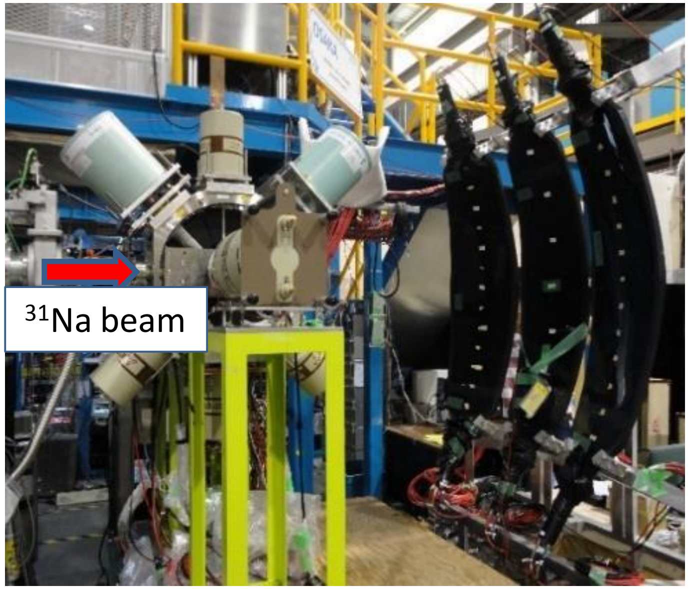

Experimental Results

β–γ measurement: $^{31}Na \rightarrow {}^{31}Mg$

Determination of polarization *P*

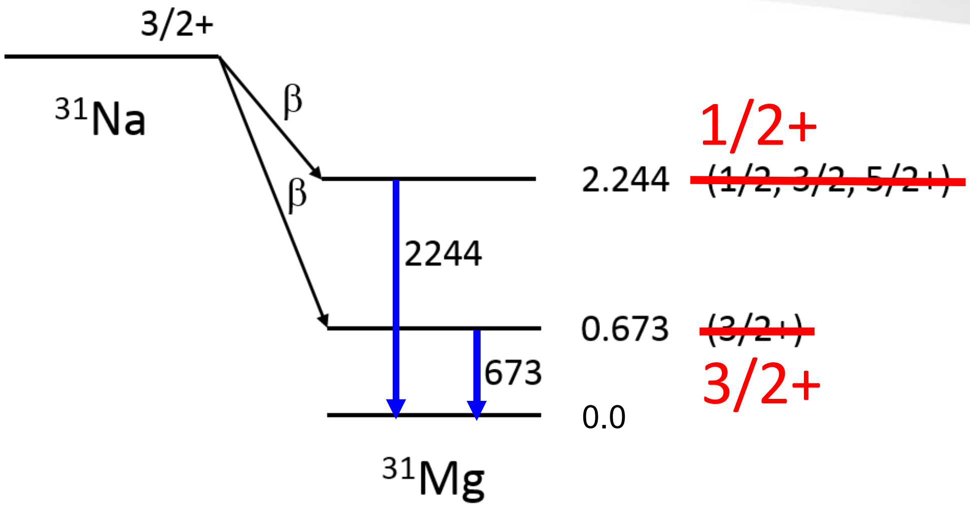

673keV γ-ray peak coincident with β-rays

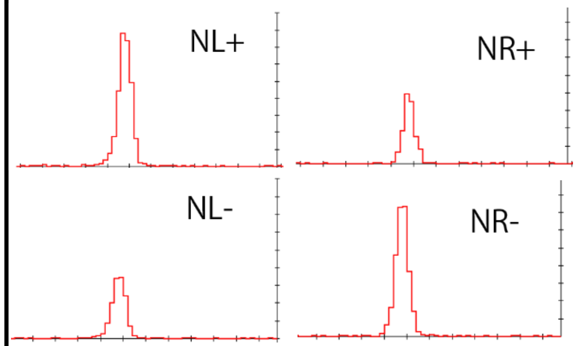

$A_{0.673}P$ = -0.11(1)

in the same manner

$A_{2.244}P$ = -0.33(1)

ratio of two *AP* values to cancel out *P*

($A_{2.244}P$)/ ($A_{0.673}P$) = $A_{2.244}$/ $A_{0.673}$ = 3.0(3)

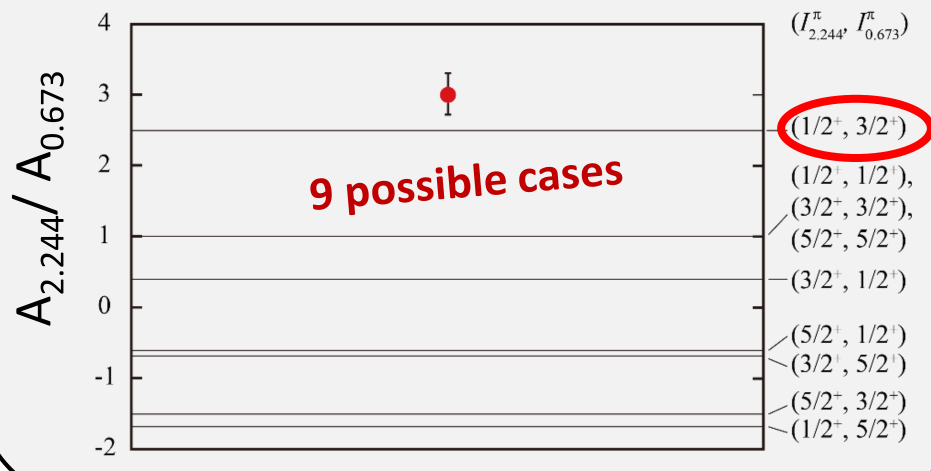

$I^{\pi}_{0.673}$ = 3/2+ ⇨ $A_{0.673}$ = -0.4

$I^{\pi}_{2.244}$ = 1/2+ ⇨ $A_{2.244}$ = -1.0

$A_{0.673}P$ = -0.11(1) ⇨ *P* = 28(3) %

$A_{2.244}P$ = -0.33(1) ⇨ *P* = 33(1) %

***P* = 32(1)%**

Spin-parity assignments of ^{31}Mg levels

experimental *AP* values and polarization $P = 32(1)\%$ ➡ *A*

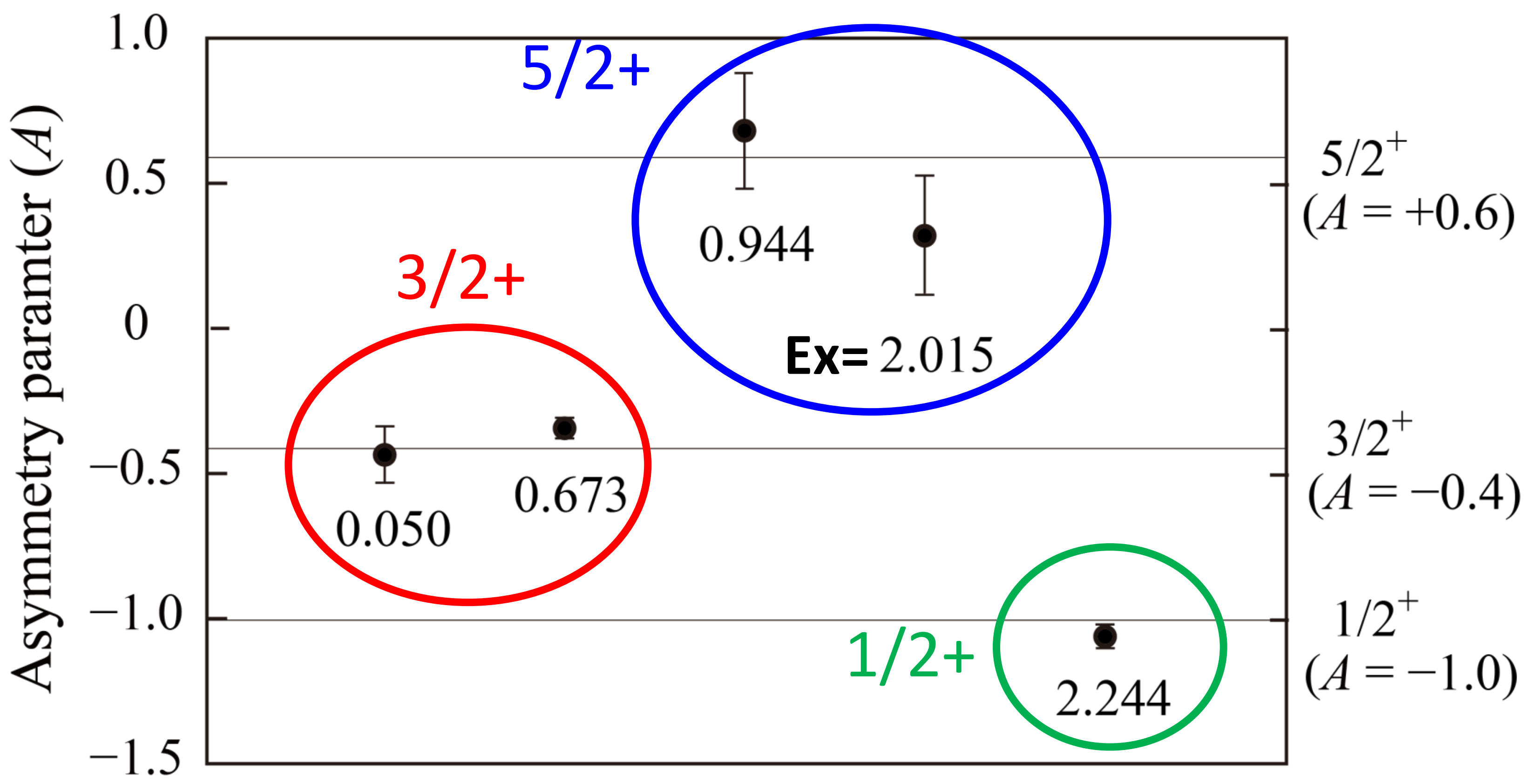

5 levels are firmly assigned!

The 50 keV level was assigned as 3/2+ for the first time.

Decay scheme of $^{31}Na \rightarrow {}^{31}Mg$

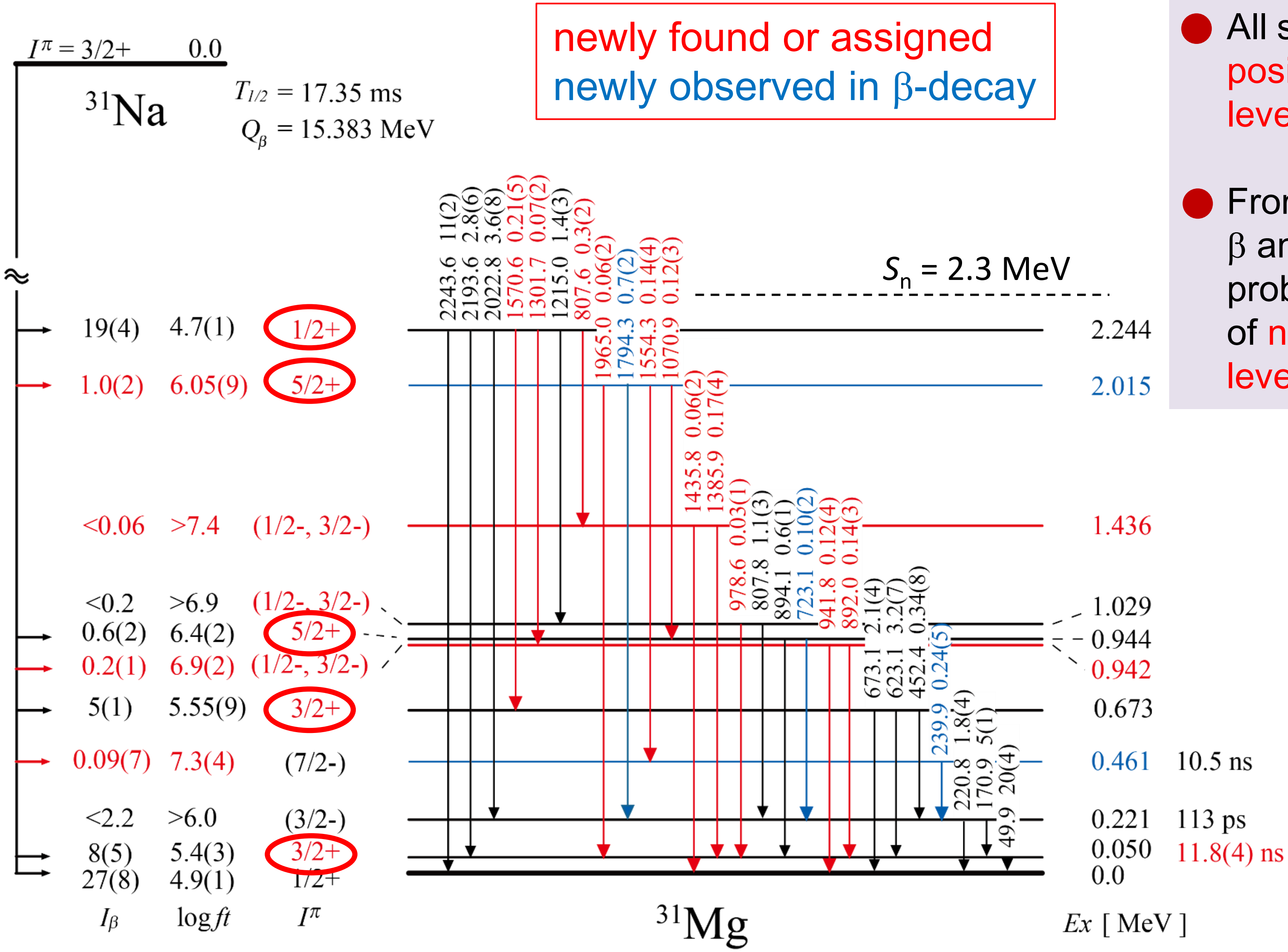

- All spins of the positive-parity levels are assigned.
- From the detailed β and γ transition probabilities, spins of negative parity-levels are proposed.

Comparison with predictions by Antisymmetrized Molecular Dynamics (AMD+GCM) theory

Comparison of energy levels

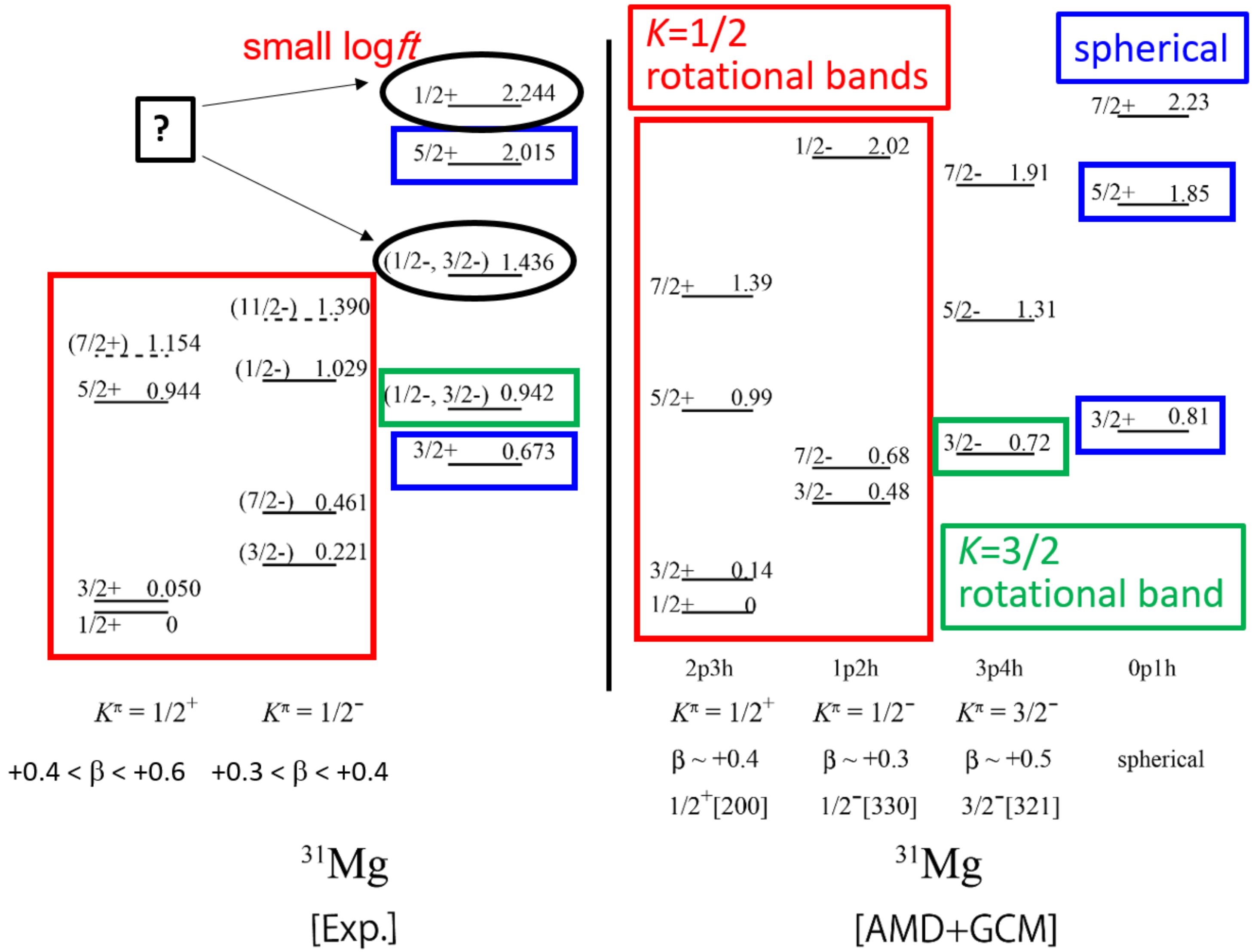

Summary

- We confirmed three types of rotational bands and spherical states.
- This is the experimental evidence of the coexistence of various structures.

Coexistence of various structures !

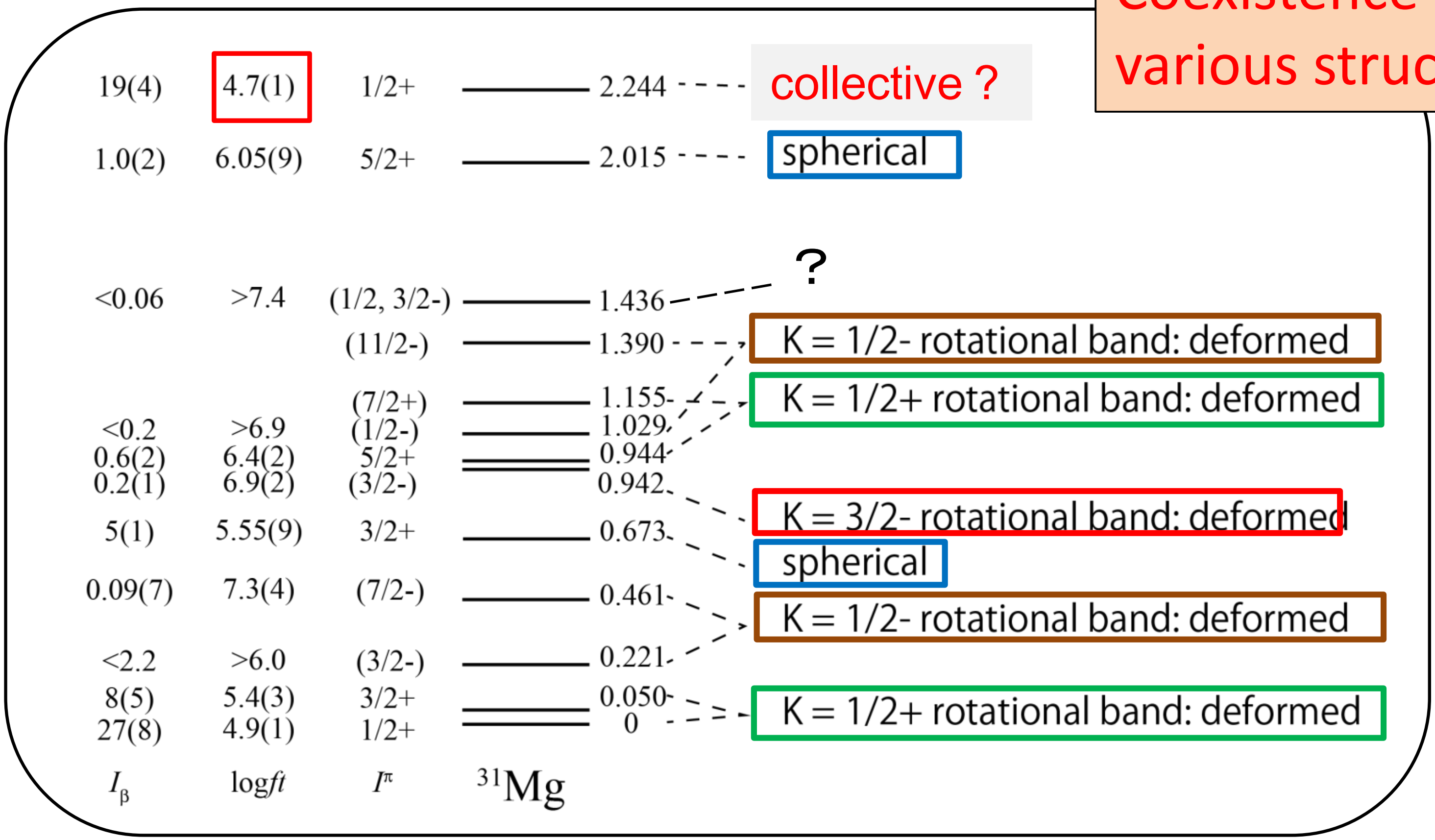

Collaborators of TRIUMF experiment S1391 (Aug. 2014)

Osaka University, Japan
H. Nishibata, T. Shimoda, A. Odahara, S. Morimoto, S. Kanaya, Y. Yagi, H. Kanaoka

TRIUMF, Canada
M. Pearson, C. D. P. Levy

Thank you for your attention.

End of presentation

Optical Pumping

alkali atom

without hyperfine int.

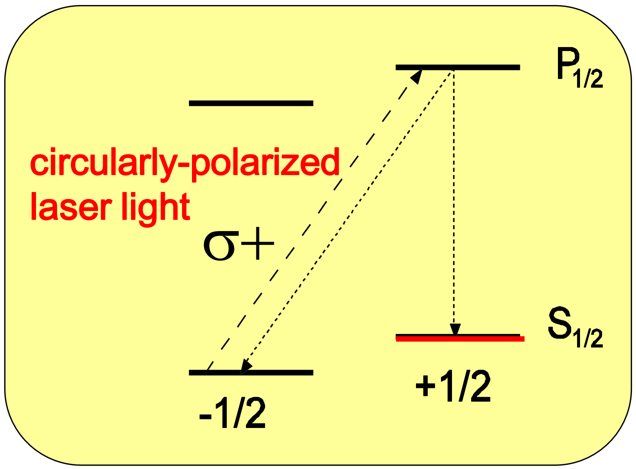

atomic polarization

with hyperfine int.

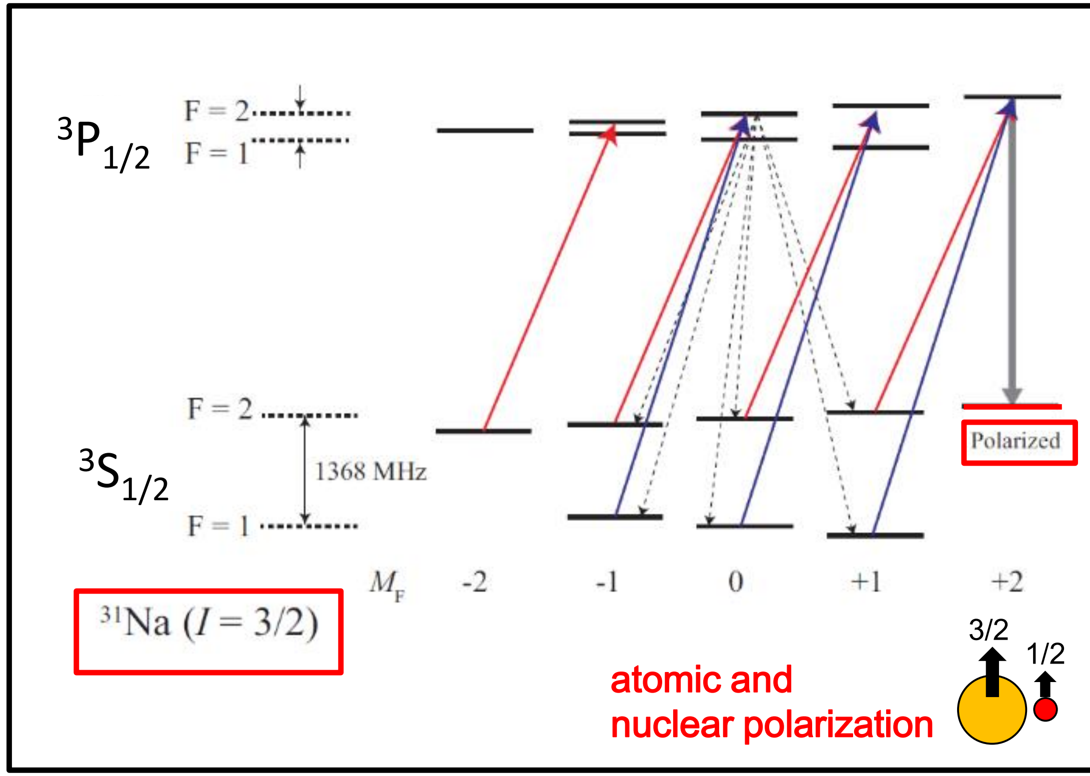

To achieve high polarization
we need two laser beams.

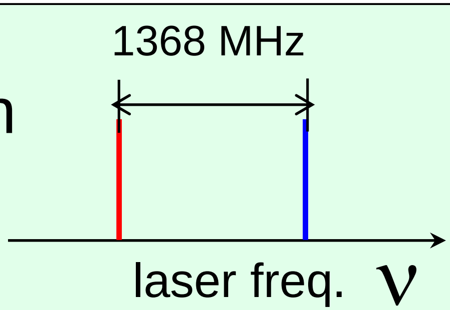

How to assign spin-parity of ^{31}Mg states

High polarization is essential
for radioactive nuclear beams.

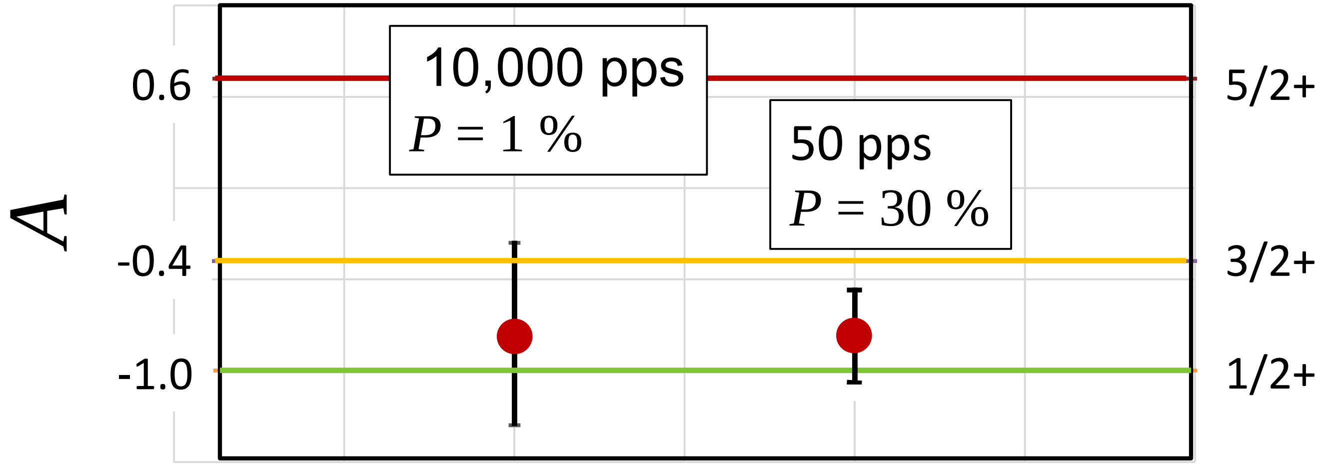

β-branch: 1%, γ-detection efficiency 1%, 24 hrs accumulation time

K=1/2 rotational bands in ^{31}Mg

Litherland et al., Can J. Phys. 36 (1958) 378

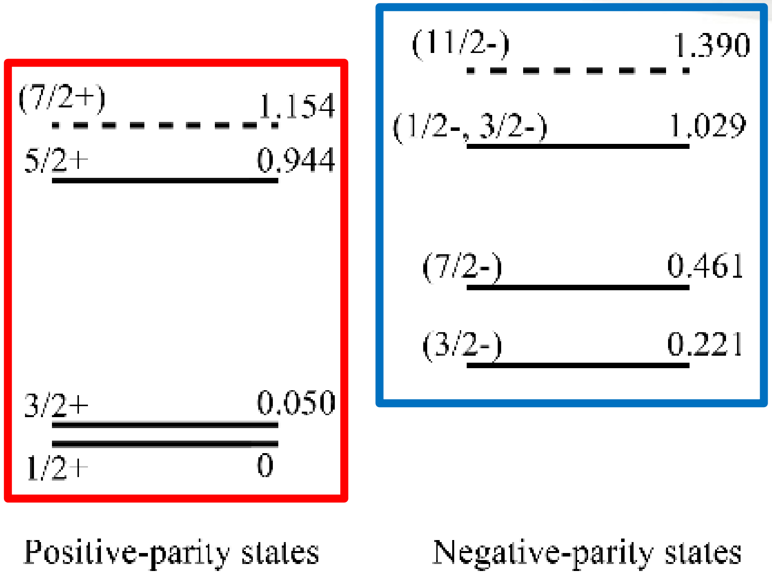

^{31}Mg

a = -0.8

K=1/2+

a = -4.4

K=1/2-

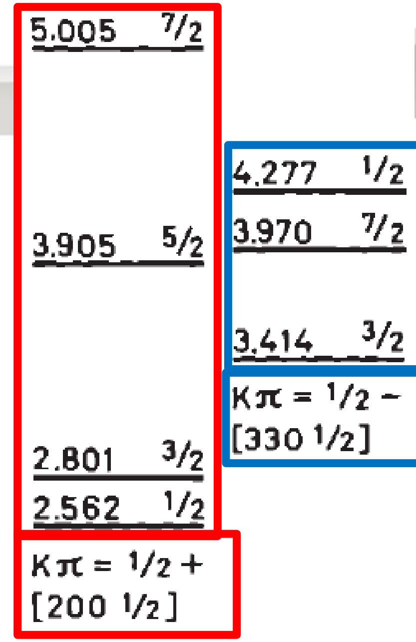

^{25}Mg

a = -0.8

K=1/2+

a = -3.5

K=1/2-

a: decoupling parameter

^{31}Mg K=1/2 rotational bands

Positive 1/2+[200] $+0.4 < \beta < +0.6$

Negative 1/2- [330] $+0.3 < \beta < +0.4$

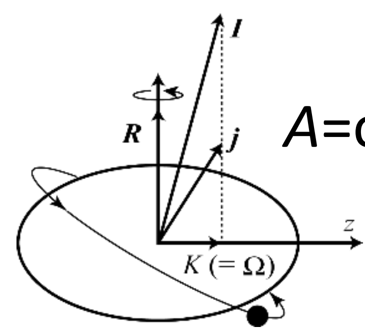

A=odd

K=1/2 rotational bands in ^{31}Mg

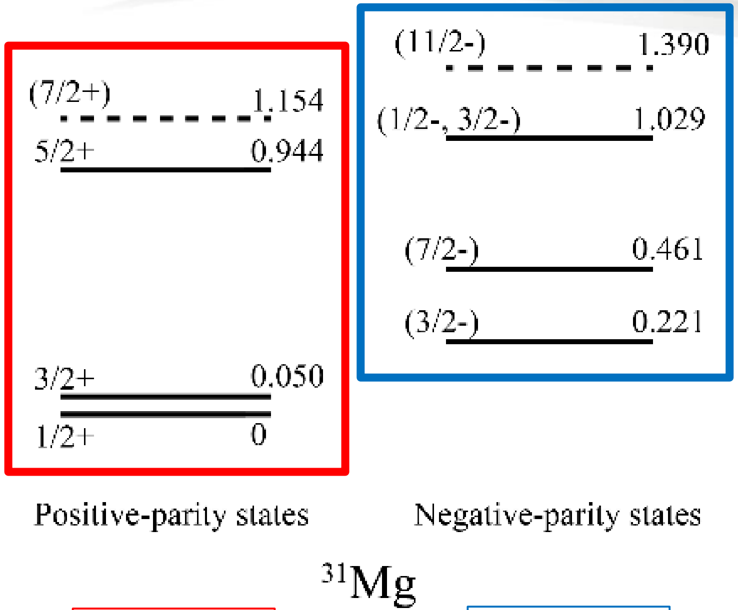

a = -0.8

a = -4.4

Decoupling parameter *a* depends on the orbit occupied by the unpaired nucleon.

Configuration could be estimated from the K=1/2 rotational band observed in ^{25}Mg.

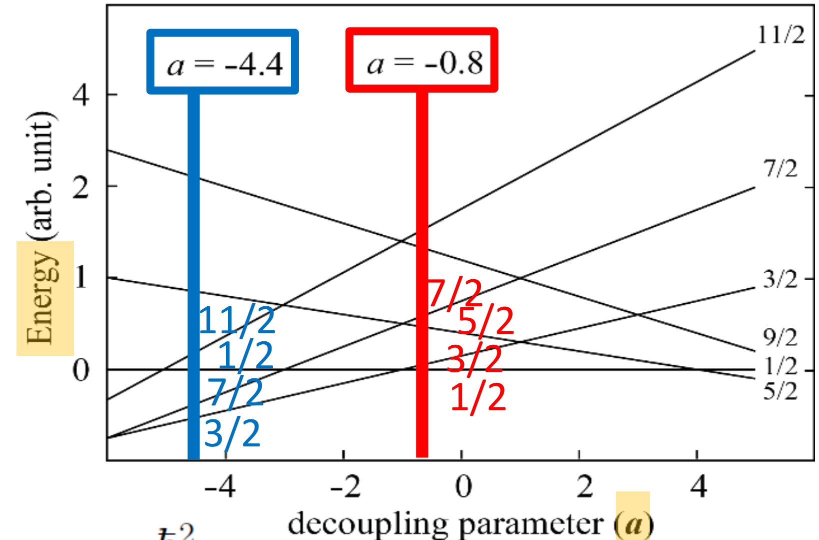

$$E(I) = \frac{\hbar^2}{2\mathcal{J}}[I(I+1) + a(-1)^{I+1/2}(I+1/2)]$$

a: decoupling parameter

from the ordering of spins
and energy difference between states

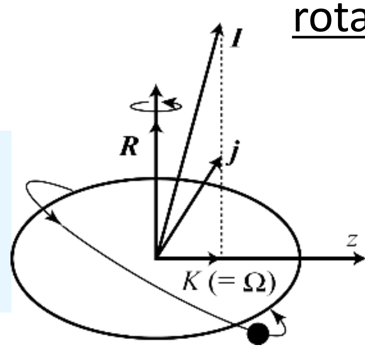

rotational motion in odd-A nuclei

- *z* : symmetry axis
- ***j*** : particle angular momentum
- ***R*** : rotational angular momentum
- ***K*** : projection of the total angular momentum on the symmetry axis
- ***I*** : total angular momentum

Litherland et al., Can J. Phys. 36 (1958) 378

K=1/2 rotational bands in ^{31}Mg

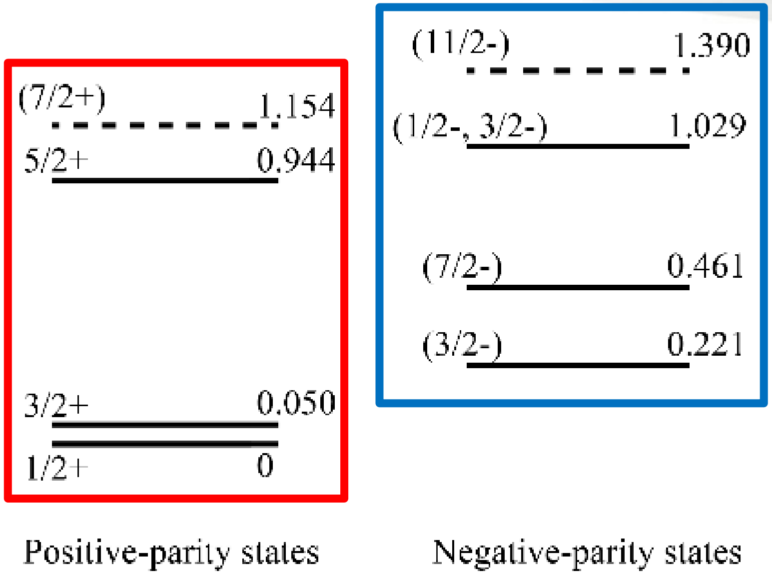

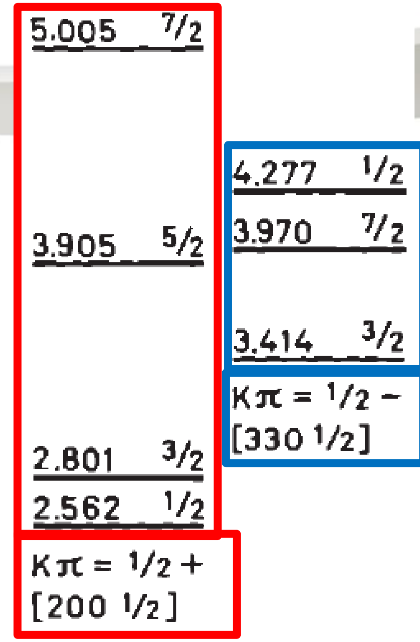

^{31}Mg

a = -0.8 K=1/2+

a = -4.4 K=1/2-

^{25}Mg

a = -0.8 K=1/2+

a = -3.5 K=1/2-

Values of decoupling parameter a
Is in good agreement with each other.

^{31}Mg *K*=1/2 rotational band
Positive 1/2+[200]
Negative 1/2- [330]

$K^{\pi}[Nn_z\Lambda]$

K^{π}: projection of the total angular momentum on the symmetry axis
N: principal quantum number
n_z: number of nodes in the wave function in the z direction
Λ: projection of the orbital angular momentum on the symmetry axis

Nilsson diagrams for ^{31}Mg

Ikuko Hamamoto, Phys. Rev. C**76** (2007) 054319

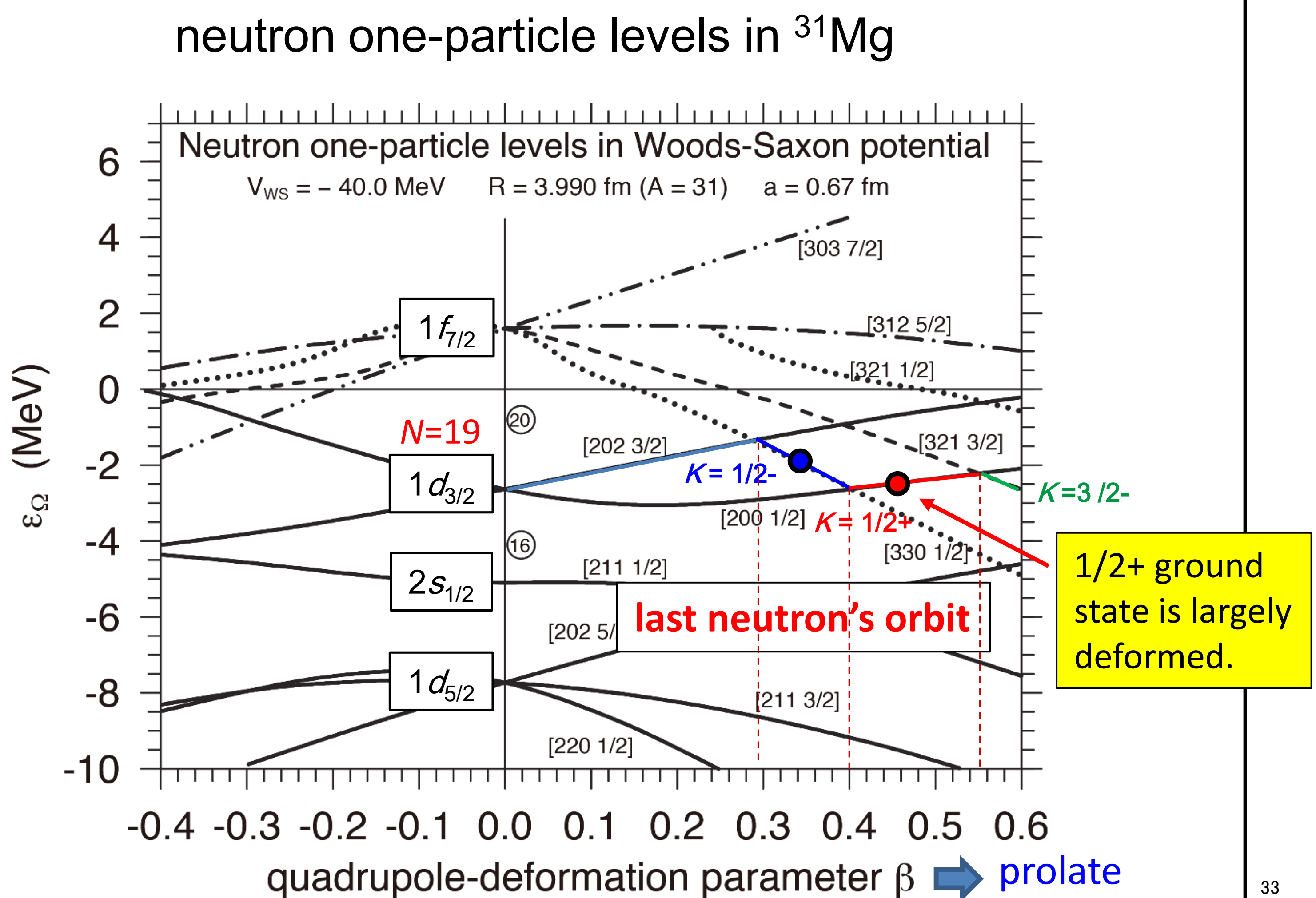

β-delayed neutrons

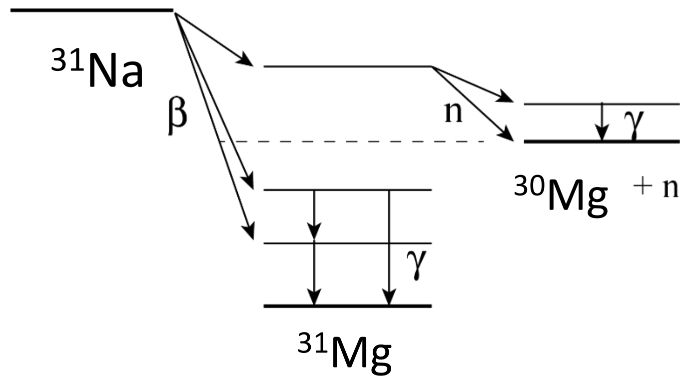

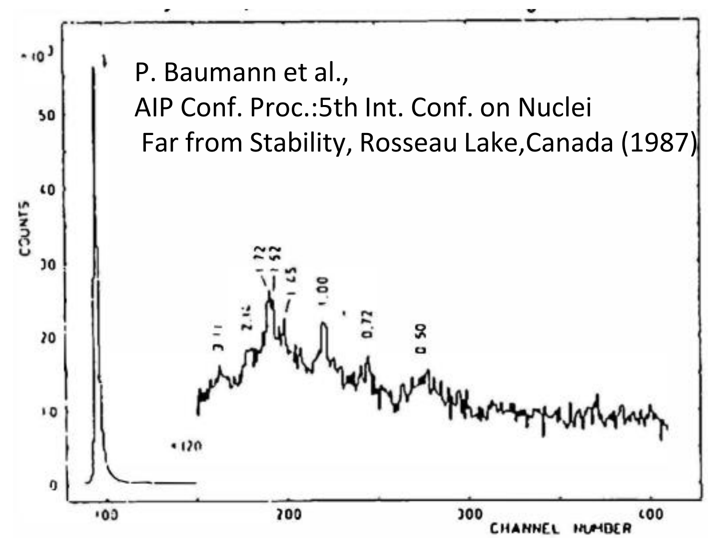

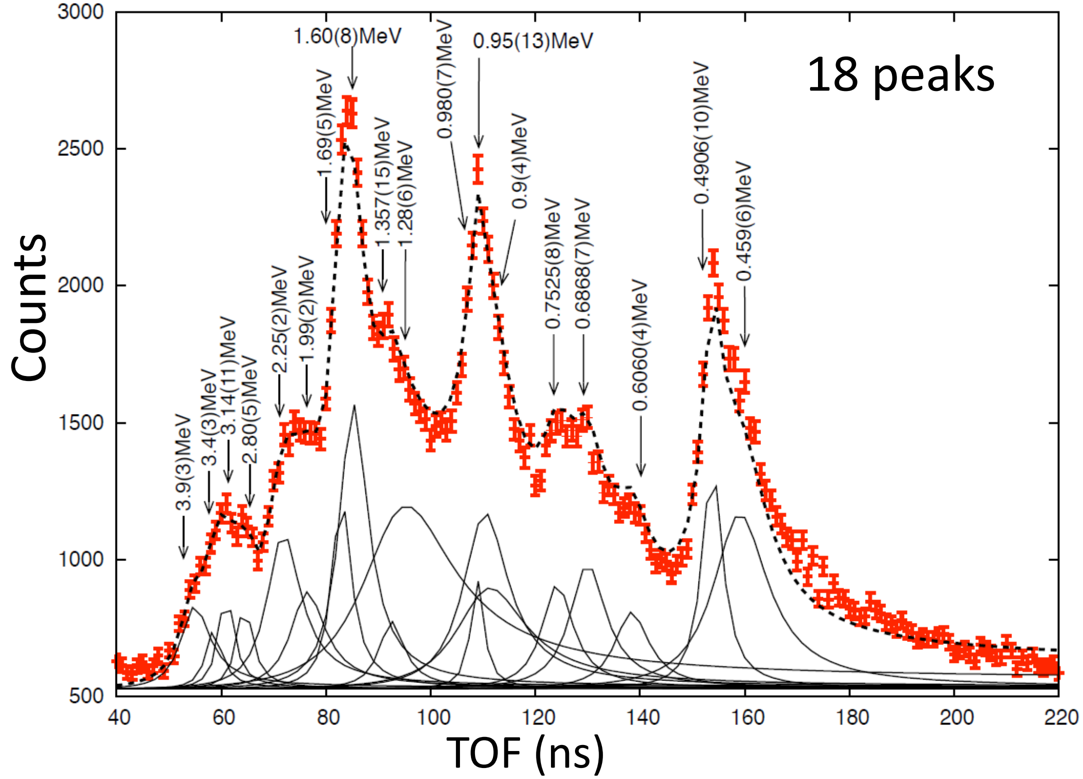

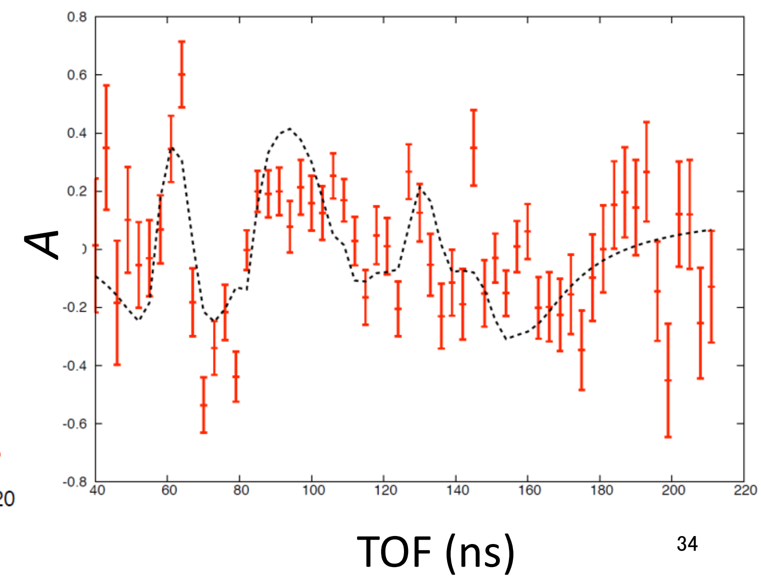

levels above S_n

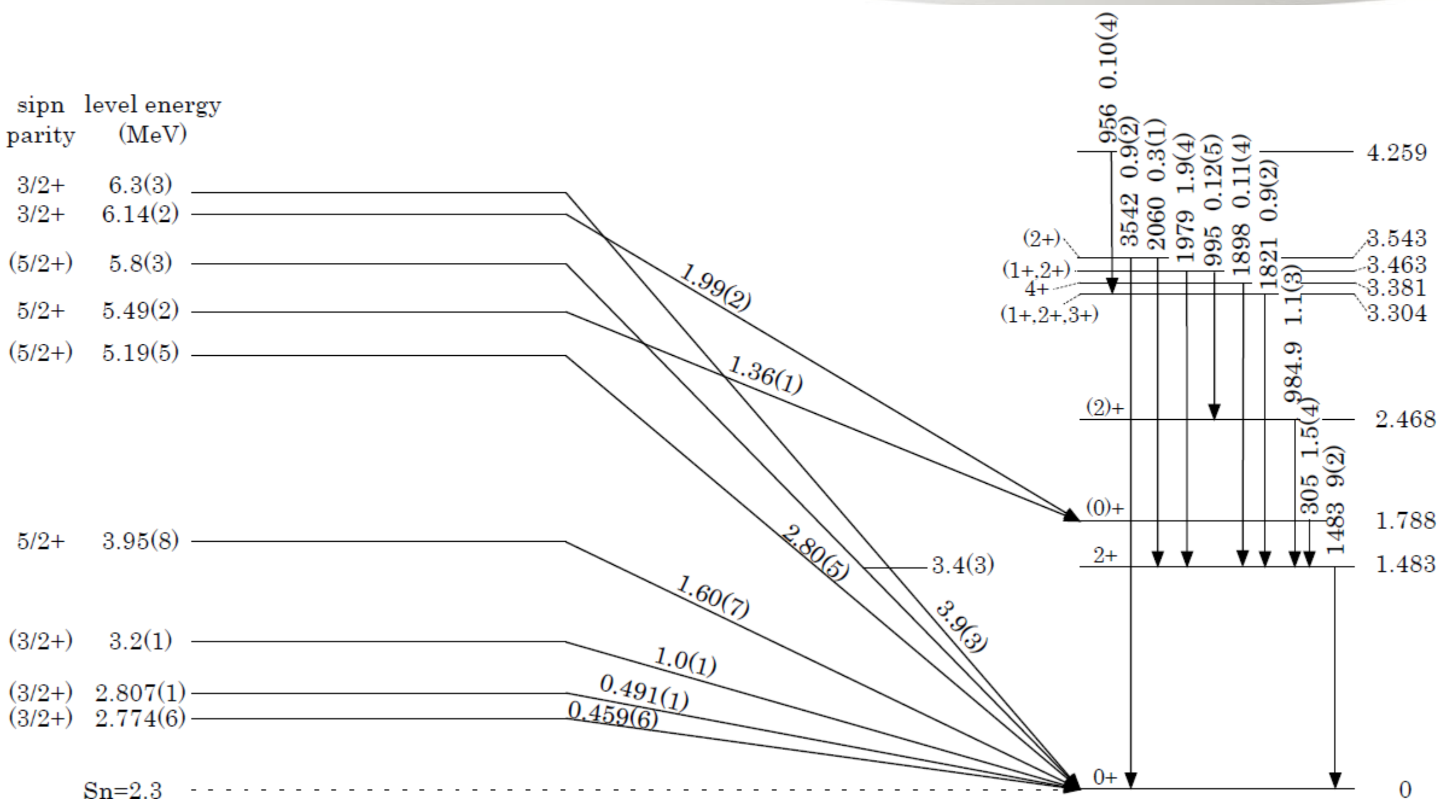

^{30}Mg

tentatively proposed

g.s.

^{31}Mg

Analysis in progress

Comparison of log*ft* values between experimental results and AMD+GCM calculation

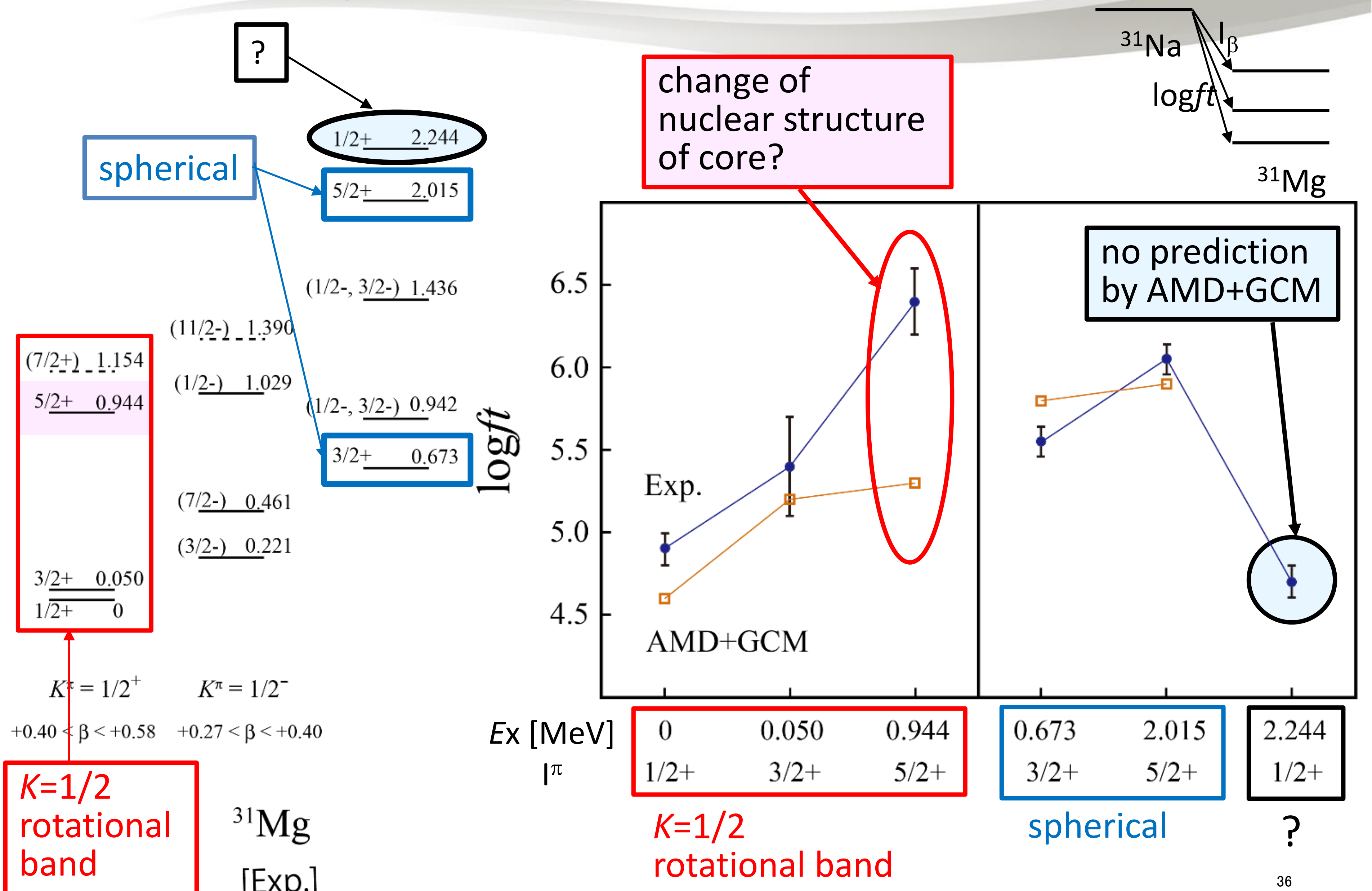

How is the level scheme of 31Mg revised?

NNDC in 2013

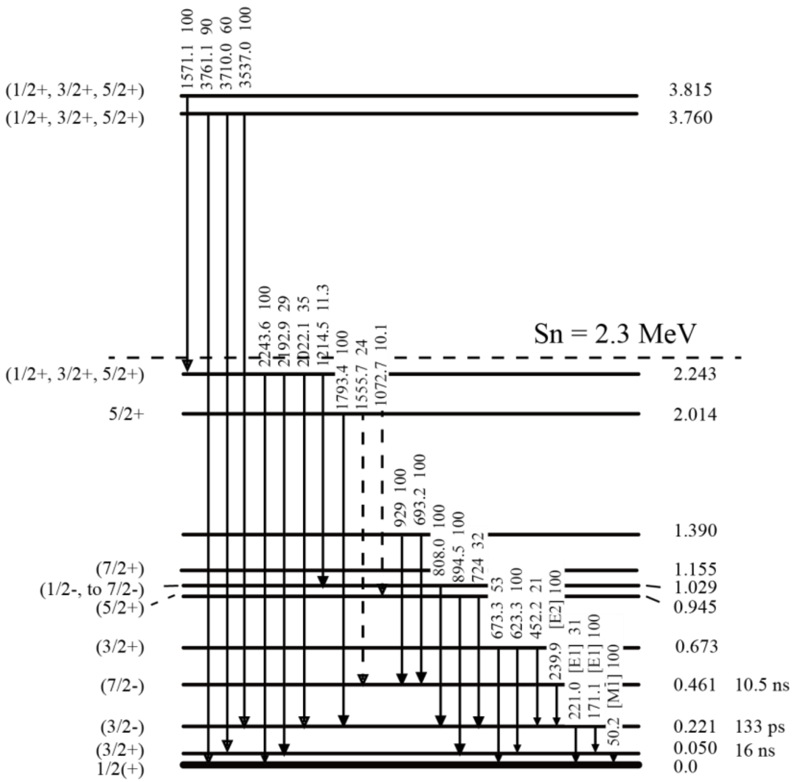

Present work
(TRIUMF experiment S1391 in 2014)

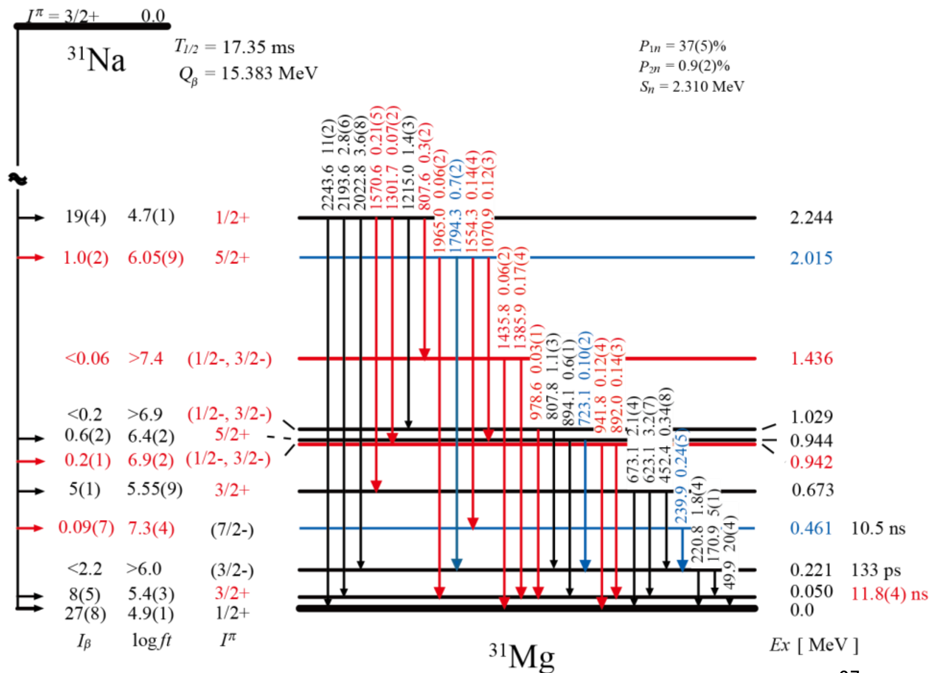

spin-parity assignment of the levels at 1.436 and 0.942 MeV

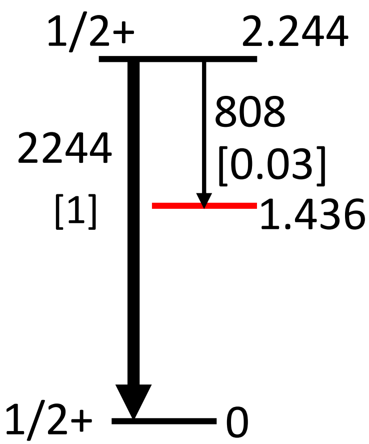

(1) 1.436-MeV level

E_γ (keV)	$E_i \to E_f$ (MeV)	I_{exp} (relative)	I^π(1.436 MeV)	$\sigma\lambda$	$T_{W.e.}(\sigma\lambda)$ (s)	$I_{W.e.}$ (relative)
2244	2.244 → g.s.	1		$M1$	2.0×10^{-15}	1
808	2.244 → 1.436	0.03(2)	$7/2^-$	$E3$	9.4×10^{-5}	2.1×10^{-11}
			$5/2^-$	$M2$	9.1×10^{-9}	2.1×10^{-7}
			$1/2^-$, $3/2^-$	$E1$	1.3×10^{-15}	6.7×10^{-1}

hindrance factor of E1 : ~10^{-2} from 2.244 ---> 0.221 MeV
(1/2+) (3/2-)

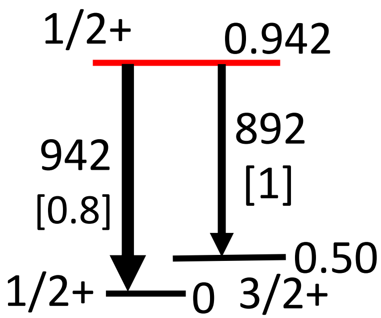

(2) 0.942-MeV level

E_γ (keV)	$E_i \to E_f$ (MeV)	I_{exp} (relative)	I^π(0.942 MeV)	$\sigma\lambda$	$T_{W.e.}(\sigma\lambda)$ (s)	$I_{W.e.}$ (relative)
892	0.942 → 0.50	1	$7/2^-$	$M2$	5.6×10^{-9}	1
942	0.942 → g.s.	0.8(3)	$7/2^-$	$E3$	3.2×10^{-5}	1.9×10^{-4}
892	0.942 → 0.50	1	$1/2^-$,$3/2^-$, $5/2^-$	$E1$	9.7×10^{-16}	1
942	0.942 → g.s.	0.8(3)	$5/2^-$	$M2$	3.4×10^{-6}	2.9×10^{-10}
			$1/2^-$, $3/2^-$	$E1$	8.2×10^{-16}	1.2×10^{0}

spin-parity assignment of the level at 1.029 MeV

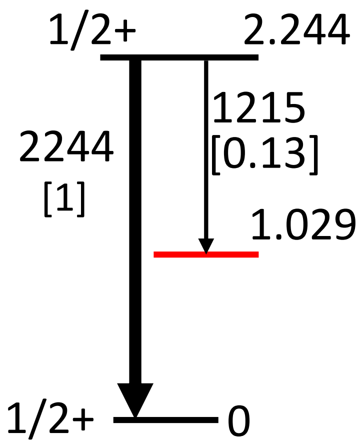

E_γ (keV)	$E_i \to E_f$ (MeV)	I_{exp} (relative)	I^π(1.436 MeV)	$\sigma\lambda$	$T_{W.e.}$ ($\sigma\lambda$) (s)	$I_{W.e.}$ (relative)
2244	$2.244 \to$ g.s.	1		$M1$	2.0×10^{-15}	1
1215	$2.244 \to 1.029$	0.13(3)	$7/2^-$	$E3$	5.4×10^{-6}	3.6×10^{-10}
			$5/2^-$	$M2$	1.2×10^{-9}	1.6×10^{-6}
			$1/2^-, 3/2^-$	$E1$	3.8×10^{-16}	5.1×10^{0}

hindrance factor of E1 : ~10^{-2} from 2.244 ---> 0.221 MeV

(1/2+) (3/2-)

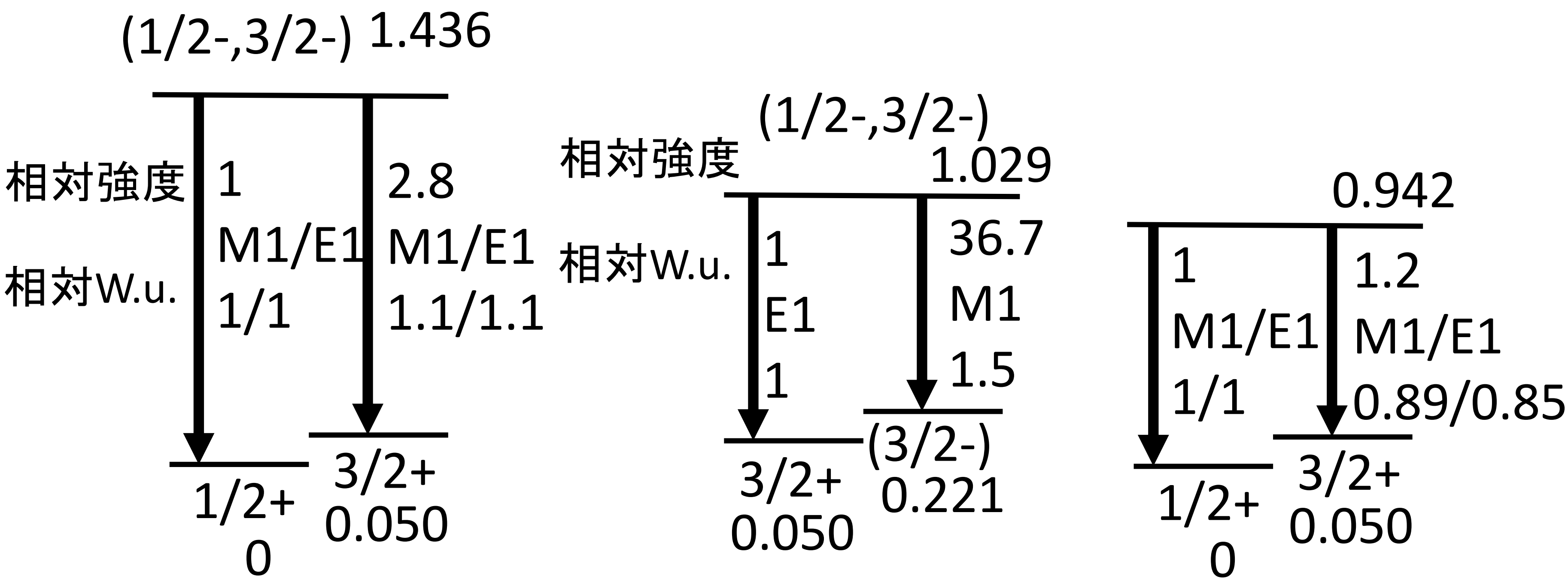
(1/2-,3/2-) 1.436
相対強度
1
2.8
M1/E1
M1/E1
相対W.u.
1/1
1.1/1.1
1/2+
0
3/2+
0.050
(1/2-,3/2-)
相対強度
1.029
相対W.u.
1
E1
1
36.7
M1
1.5
3/2+
0.050
(3/2-)
0.221
0.942
1
M1/E1
1/1
1.2
M1/E1
0.89/0.85
1/2+
0
3/2+
0.050

No such high-energy γ-rays were observed.

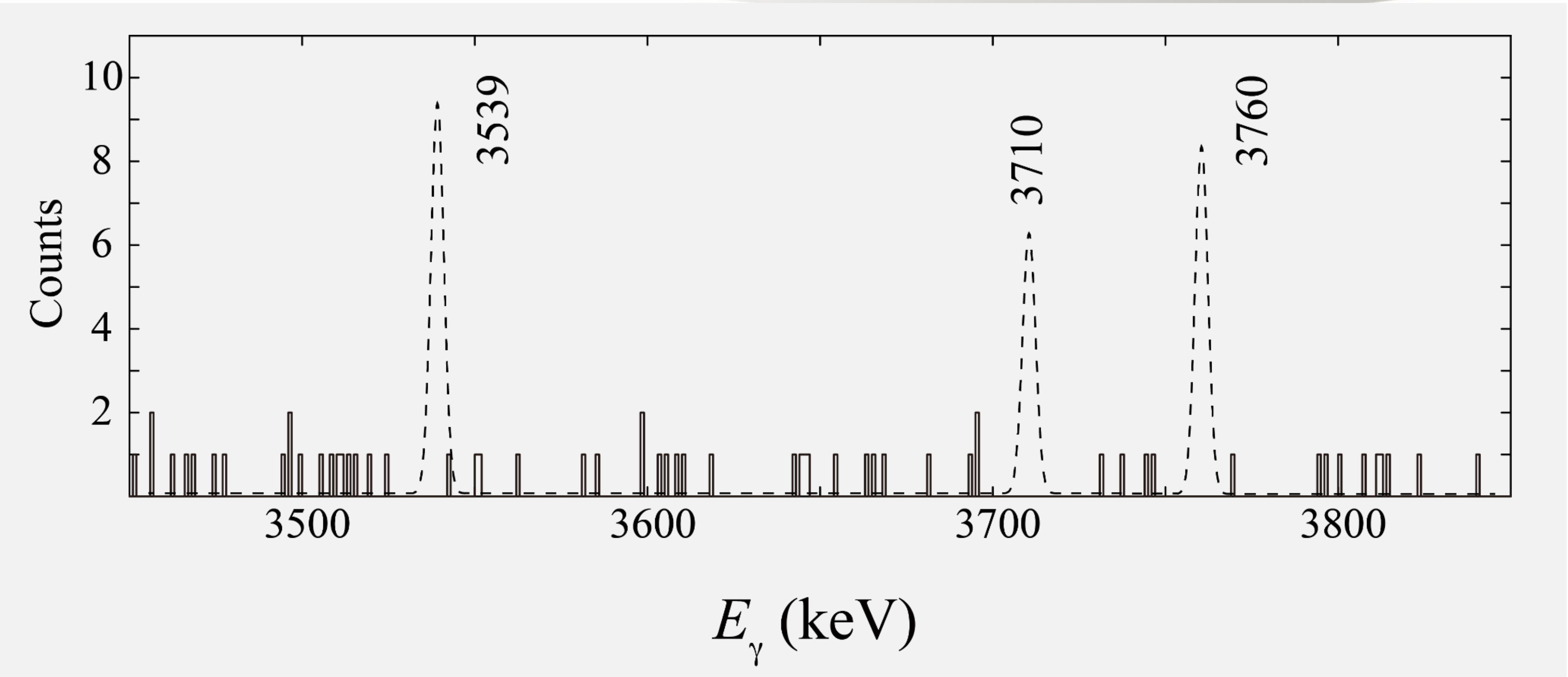

Enlarged β-γ coincidence spectrum for ^{31}Mg gated by β rays with more than 8 MeV indicated by solid line and the expected spectrum from the level scheme of Ref. [KLO93] shown in the dashed line.

Detection efficiency with β-gate is taken into account.

In the case of cascade feeding

Deduced A from β-γ coincidence is affected by the feeding from upper levels.

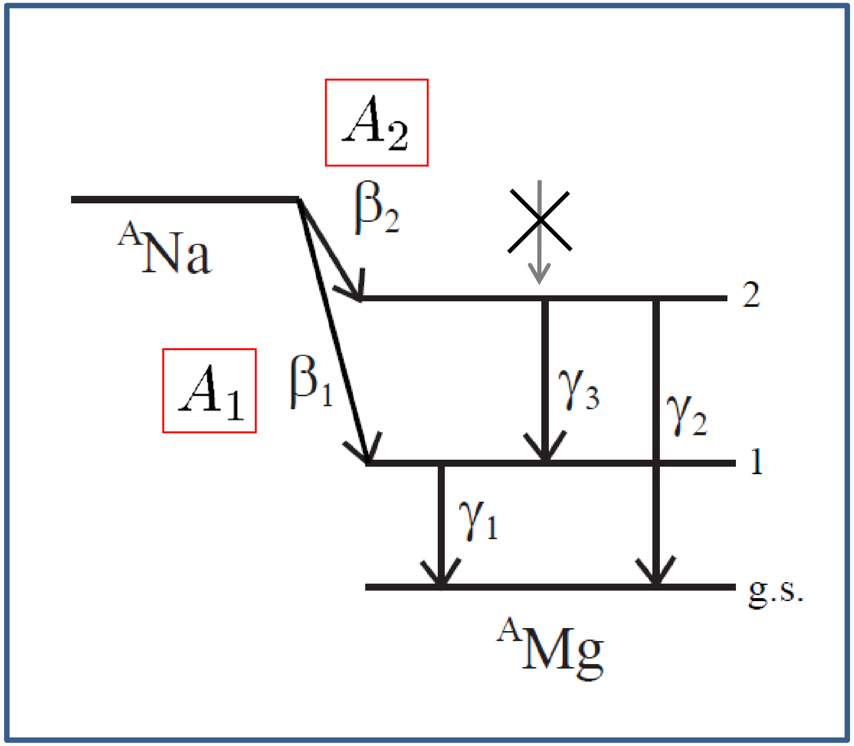

measured from β-γ_1 coincidence

$$A_1^{\gamma} = A_2 \times \frac{I_{\gamma_3}}{I_{\gamma_1}} + A_1 \times \frac{I_{\beta_1}}{I_{\gamma_1}},$$

known — unknown

$$A_1 = A_1^{\gamma} \times \frac{I_{\gamma_1}}{I_{\beta_1}} - A_2 \times \frac{I_{\gamma_3}}{I_{\beta_1}}.$$

Achieved polarization

Phil Levy @TRIUMF

^{8}Li: 80%, ^{9}Li: 56%, ^{11}LI: 55%,

^{20}Na: 57%, ^{21}Na: 56%, ^{26}Na: 55%,
^{27}Na: 51%, ^{28}Na: 45%,

Corrected for spin-relaxation
K. Minamisonno et al.,
Nucl. Phys. A746(2004)673c

^{28}Na: 28%, ^{29}Na: 36%,
^{30}Na: 31%, ^{31}Na: 32%

Uncorrected for spin-relaxation,
attenuation due to solid angle

Spin Relaxation

Pt $B_0 = 0.5$ T

^{20}Na 22.0(19) s
^{26}Na 0.78(8) s

Korringa's relation

$T_1 \times T \propto (Ih/\mu)^2$

^{30}Na 600 ms 48 ms
^{31}Na 400 ms 17 ms

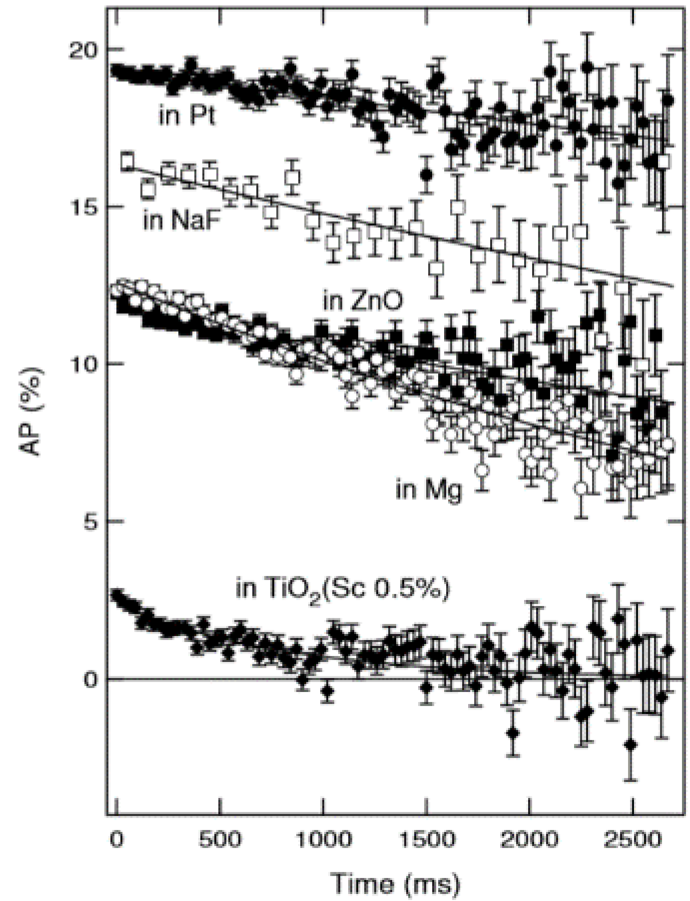

Figure 1: Time spectra of ^{20}Na polarization in several catchers.

K. Minamizono et al.
Hyperfine Interactions 159, 261 (2004)

^{31}Na β−decay

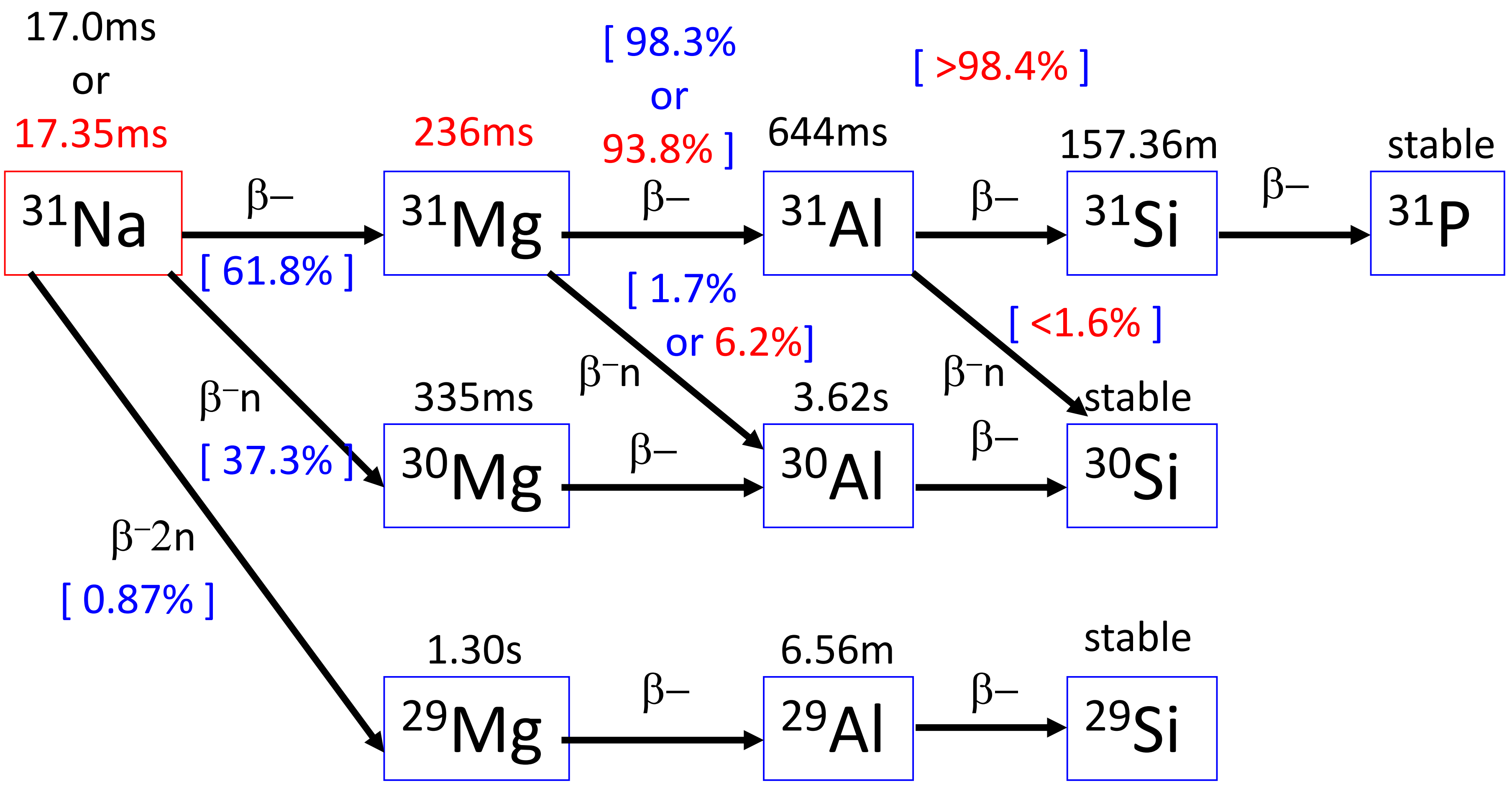
17.0ms
or
17.35ms
31Na
β–
[61.8%]
236ms
31Mg
[98.3%
or
93.8%]
β–
644ms
31Al
[>98.4%]
β–
157.36m
31Si
β–
stable
31P
[1.7%
or 6.2%]
β⁻n
[<1.6%]
β⁻n
β⁻n
[37.3%]
335ms
30Mg
β–
3.62s
30Al
β–
stable
30Si
β⁻2n
[0.87%]
1.30s
29Mg
β–
6.56m
29Al
β–
stable
29Si

TRIUMF Mass separator

TRIUMF Mass separator

$\Delta M/M \sim 1/10000$

^{31}Na-^{31}Mg $\Delta M/M \sim 1/1825$

^{31}Na-^{31}Al $\Delta M/M \sim 1/1050$

energy (Doppler) broadening of the neutralized beam

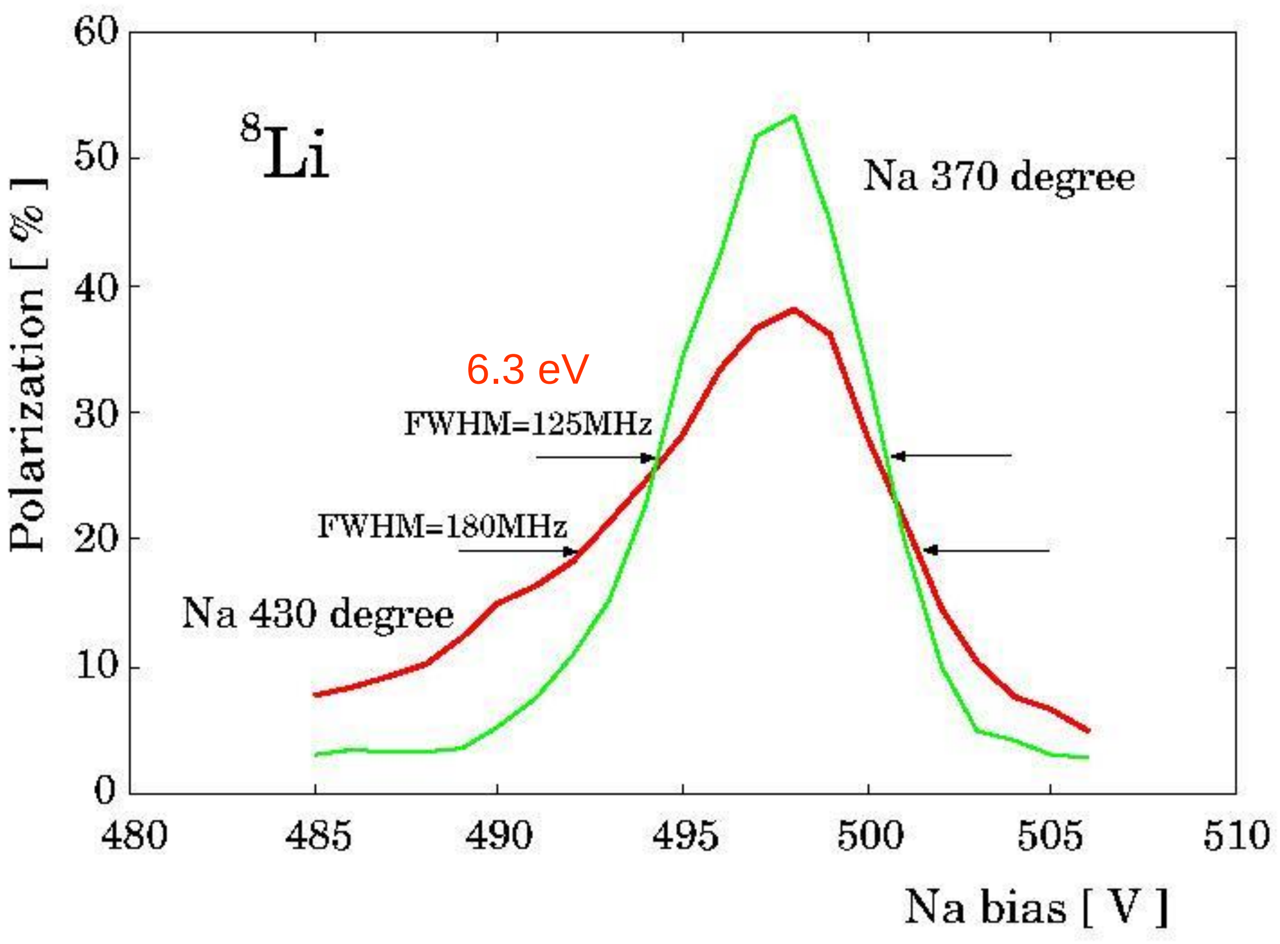

>> laser line width
～ 1 MHz

multiple collisions with Na atoms in the neutralizer

Beam tuning

共鳴点のサーチ

Na cellのvoltageをかえる

(a)

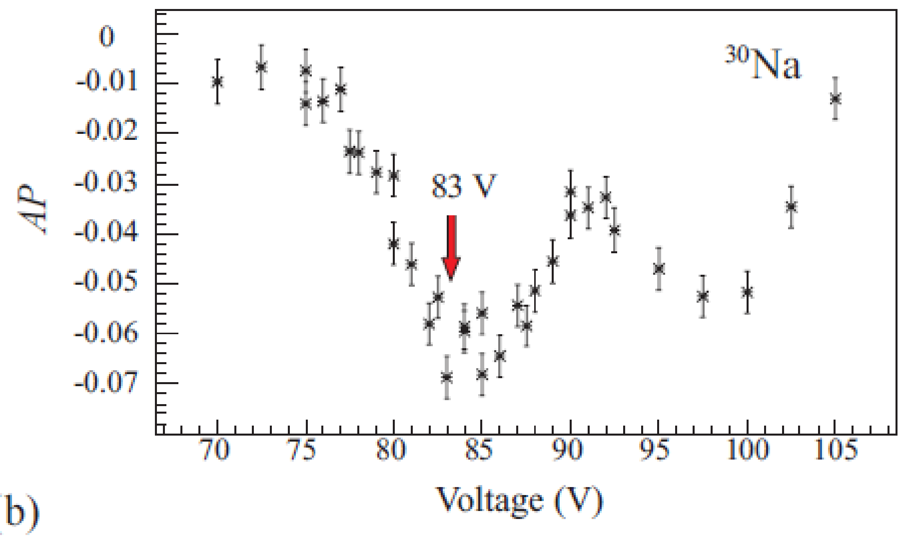

(b)

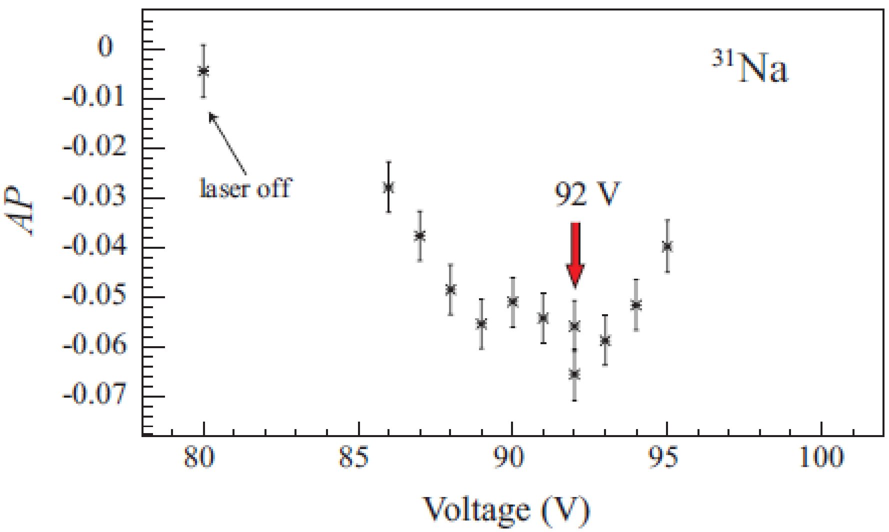

Doppler-shift tuning

deceleration bias (Na vapor cell) tuning to adjust ion beam velocity so as to meet the Doppler shift

beta-decay asymmetry

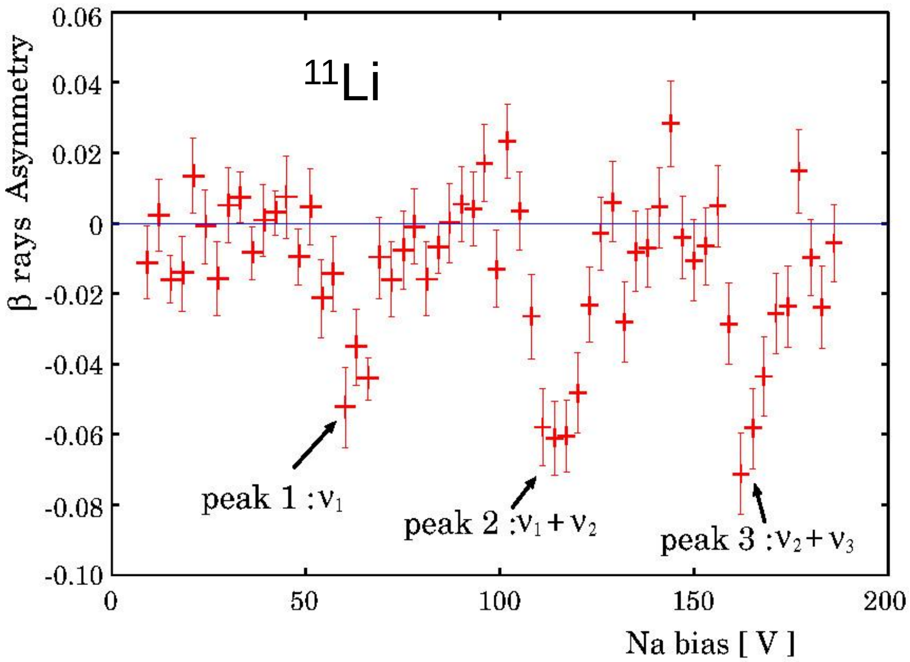

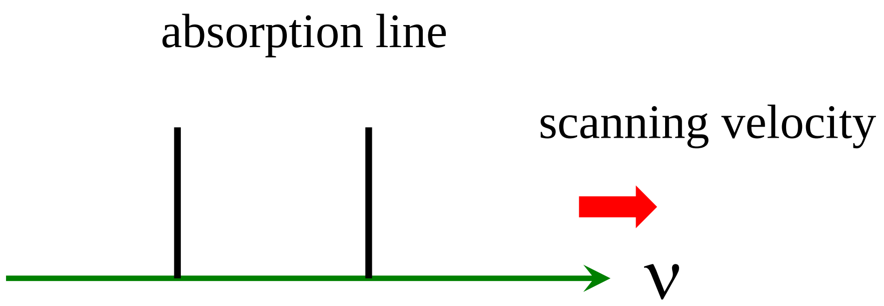

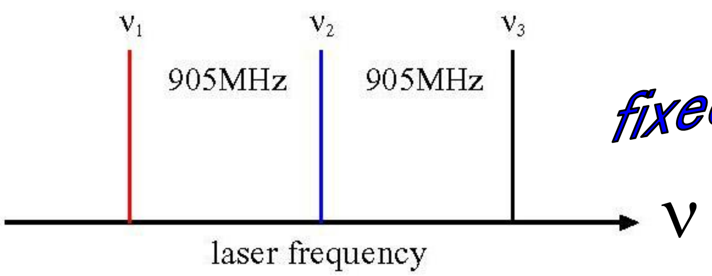

fixed

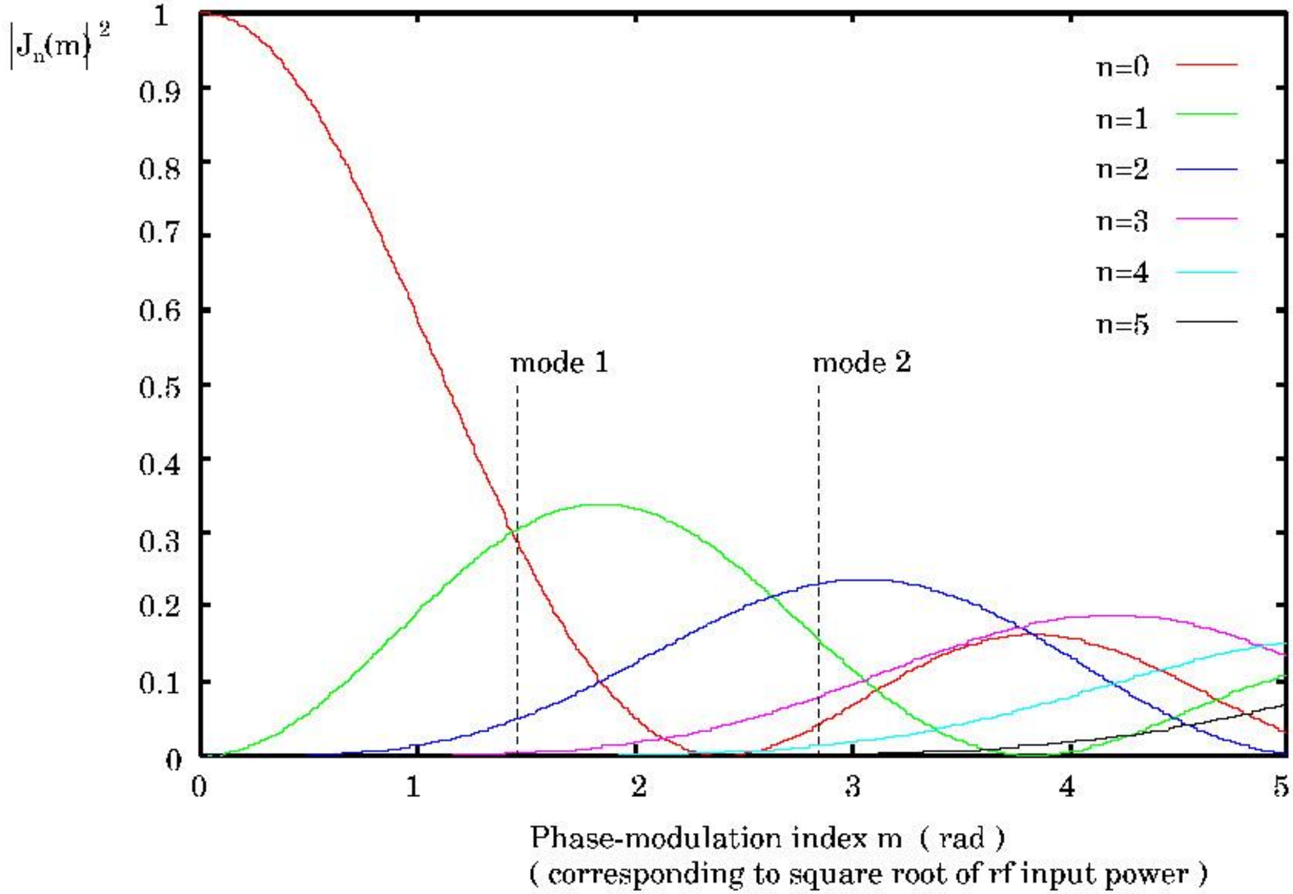
$|J_n(m)|^2$
n=0
n=1
n=2
n=3
n=4
n=5
mode 1
mode 2
Phase-modulation index m (rad)
(corresponding to square root of rf input power)

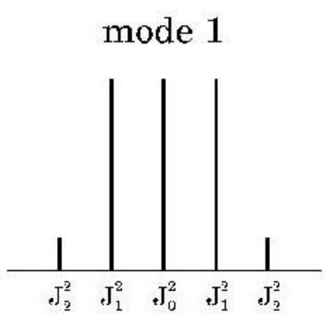
mode 1
J_2^2 J_1^2 J_0^2 J_1^2 J_2^2

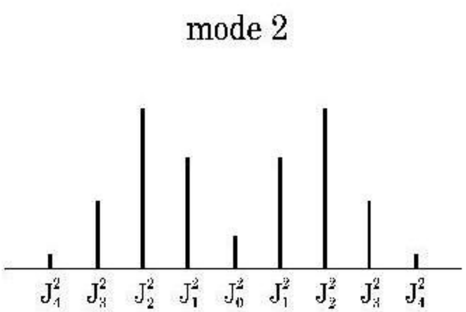
mode 2
J_4^2 J_3^2 J_2^2 J_1^2 J_0^2 J_1^2 J_2^2 J_3^2 J_4^2

Comparison with shell model calculation

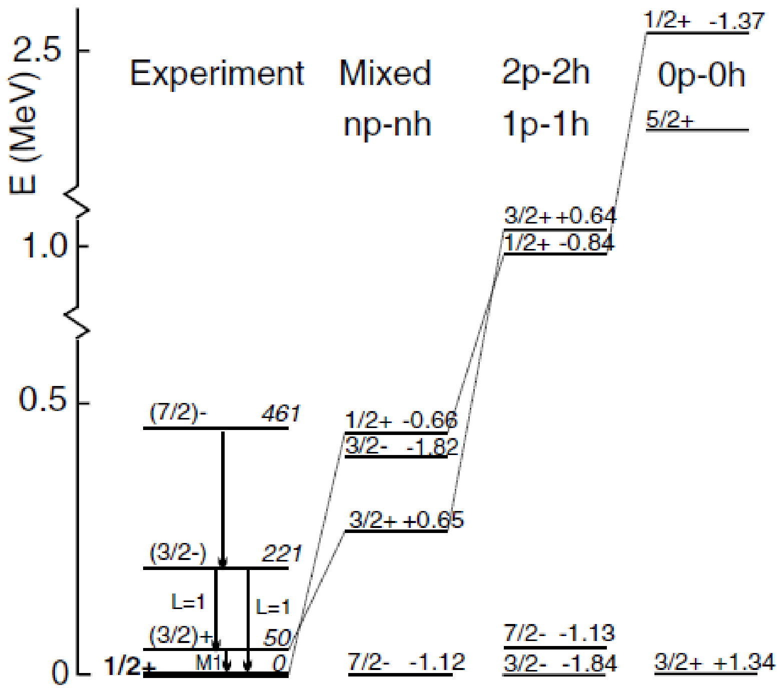

G. Neyens et al., Phys. Rev. Lett. 94, 022501(2005)

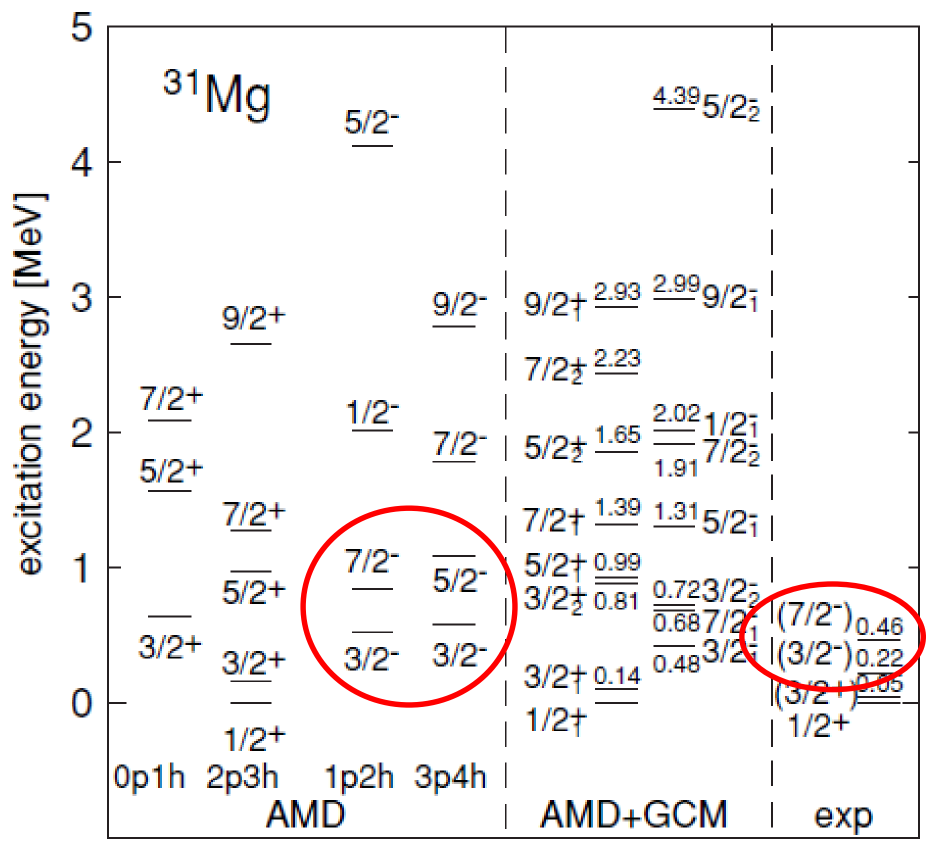

M. Kimura, Phys. Rev. C75, 041302(R) (2007)

spin-parity of the ground state in ^{31}Mg : understanding from the shell model

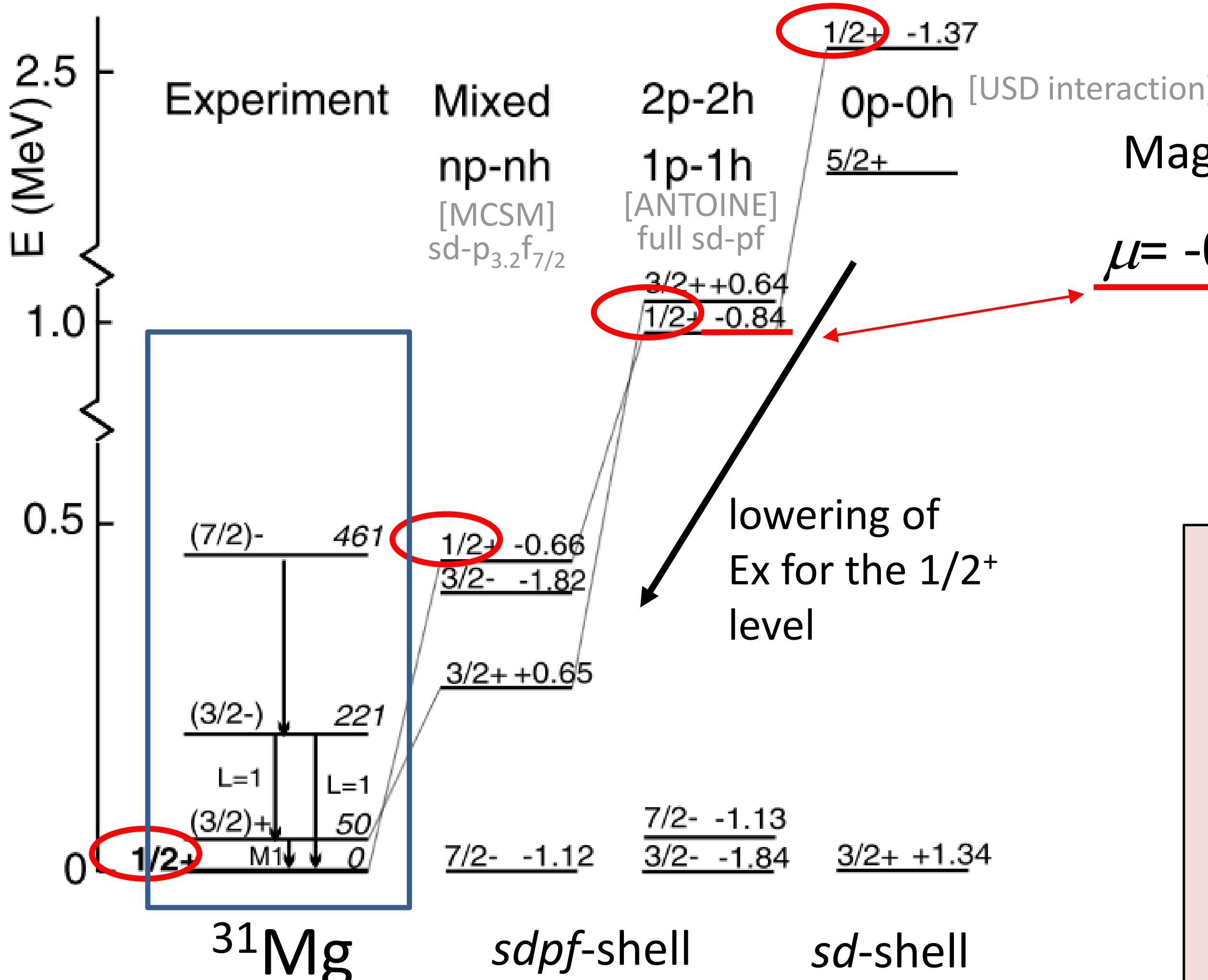

Magnetic moment

μ= -0.88355(15) μ_N

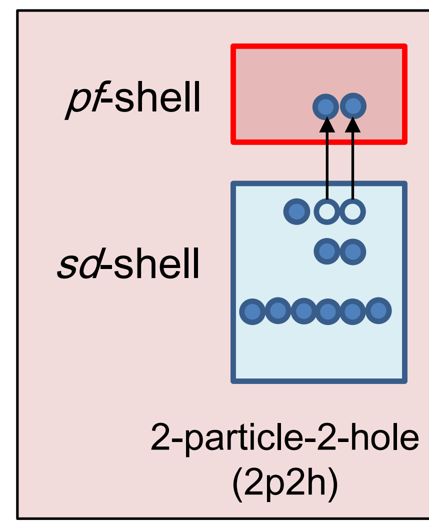

G. Neyens et al., Phys. Rev. Lett. 94, 022501 (2005)

Negative-parity states in ^{31}Mg

Lifetime measurement in ^{31}Na β decay

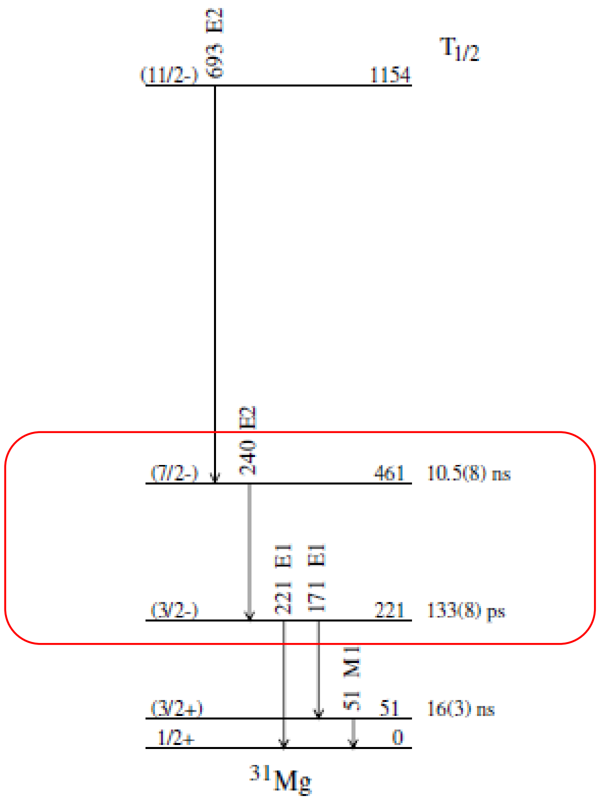

Fig. 2. A partial level scheme of ^{31}Mg and preliminary level lifetimes established in this work, except for the 51 keV level, which is taken from [2]. The suggested spin/parity assignments for the excited levels and transition multipolarities are model dependent [2] although supported by the observed transition rates.

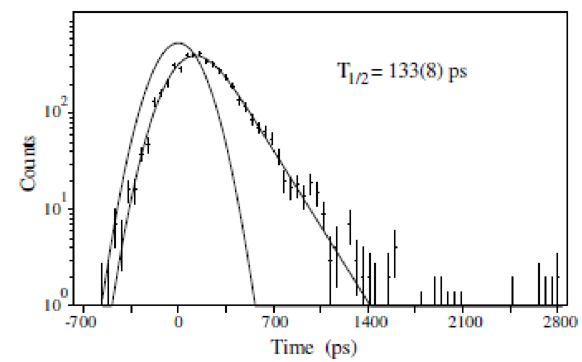

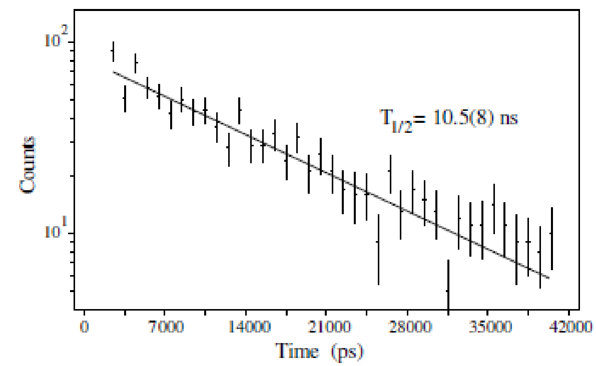

BaF$_2$ detector

H. Mach et al., Eur. Phys. J. A 25 s01, 105 (2005).

anti-symmetrized molecular dynamics plus generator coordinate method (AMD+GCM)

AMD Antisymmetrized Molecular Dynamics

Reasonably describes cluster states such as ^{12}Be

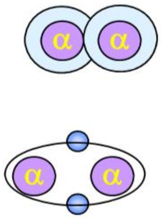

Y. Kanada-En'yo et al.,
Phys. Rev. C 68, 014319 (2003)

A Slater determinant of single particle wave packets.

$$\Phi_{\rm int} = \frac{1}{\sqrt{A!}} \det\{\varphi_i(\mathbf{r}_j)\}$$

$$\varphi_i(\mathbf{r}) = \phi_i(\mathbf{r}) \cdot \chi_i \cdot \xi_i$$

spatial: $\phi_i(\mathbf{r}) = \exp\{-(\mathbf{r}-\mathbf{Z}_i)\mathbf{M}(\mathbf{r}-\mathbf{Z}_i)\}$

spin: $\chi_i = \alpha_i \chi_\uparrow + \beta_i \chi_\downarrow$

isospin: $\xi_i =$ proton or neutron

$$\hat{H} = \hat{T} - \hat{T}_g + \hat{V}_{\rm Gogny} + \hat{V}_{\rm Coulomb}$$

GCM Generator Coordinate Method

treats collective motion

Theoretical Framework of AMD+GCM

Wave function of AMD

Variational wave function:

The parity is projected before the variation.

$$\Phi^\pi = \hat{P}^\pi \Phi_{\rm int}$$

Intrinsic wave function:

A Slater determinant of single particle wave packets.

$$\Phi_{\rm int} = \frac{1}{\sqrt{A!}} \det\{\varphi_i(\mathbf{r}_j)\}$$

$$\varphi_i(\mathbf{r}) = \phi_i(\mathbf{r}) \cdot \chi_i \cdot \xi_i$$

spatial: $\phi_i(\mathbf{r}) = \exp\{-(\mathbf{r}-\mathbf{Z}_i)\mathbf{M}(\mathbf{r}-\mathbf{Z}_i)\}$

spin: $\chi_i = \alpha_i \chi_\uparrow + \beta_i \chi_\downarrow$

isospin: $\xi_i =$ proton or neutron

Variational parameters:

size and deformation of Gaussian $\mathbf{M}$:
3x3 real sym. matrix

centroinds of Gaussian $\mathbf{Z}_i (i=1,\ldots,A)$:
complex 3d vectors

direction of spin α_i and β_i $(i=1,\ldots,A)$:
complex numbers

Variation after parity projection

Hamiltonian and energy:

$$\hat{H} = \hat{T} - \hat{T}_g + \hat{V}_{\rm Gogny} + \hat{V}_{\rm Coulomb}$$

$$E^{J\pi}_{MK} = \langle \Phi^{J\pi}_{MK} | \hat{H} | \Phi^{J\pi}_{MK} \rangle / \langle \Phi^{J\pi}_{MK} | \Phi^{J\pi}_{MK} \rangle$$

Frictional cooling method:

$$\dot{X}_i = (\mu + i\nu) c_{ij} \frac{\partial E^{J\pi}_{MK}}{\partial X_j}$$

Ang. Mom. Proj. and GCM

Ang. Mom. Proj.:

$$\Phi^{J\pi}_{MK}(m^{\rm th}) = \hat{P}^J_{MK} \Phi^\pi(m^{\rm th})$$

GCM:

$$\Psi^{J\pi}_\alpha = \sum_{m=1}^{n} f^\alpha_m \Phi^{J\pi}_{MK}(m^{\rm th})$$

$$(H_{mm'} - E^\alpha N_{mm'}) f^\alpha_{m'} = 0$$

$$H_{mm'} = \langle \Phi^{J\pi}_{MK}(m^{\rm th}) | \hat{H} | \Phi^{J\pi}_{MK}(m'^{\rm th}) \rangle,$$

$$N_{mm'} = \langle \Phi^{J\pi}_{MK}(m^{\rm th}) | \Phi^{J\pi}_{MK}(m'^{\rm th}) \rangle$$

Excited States in even-mass Mg isotopes

Examples: 0+ states with different shapes

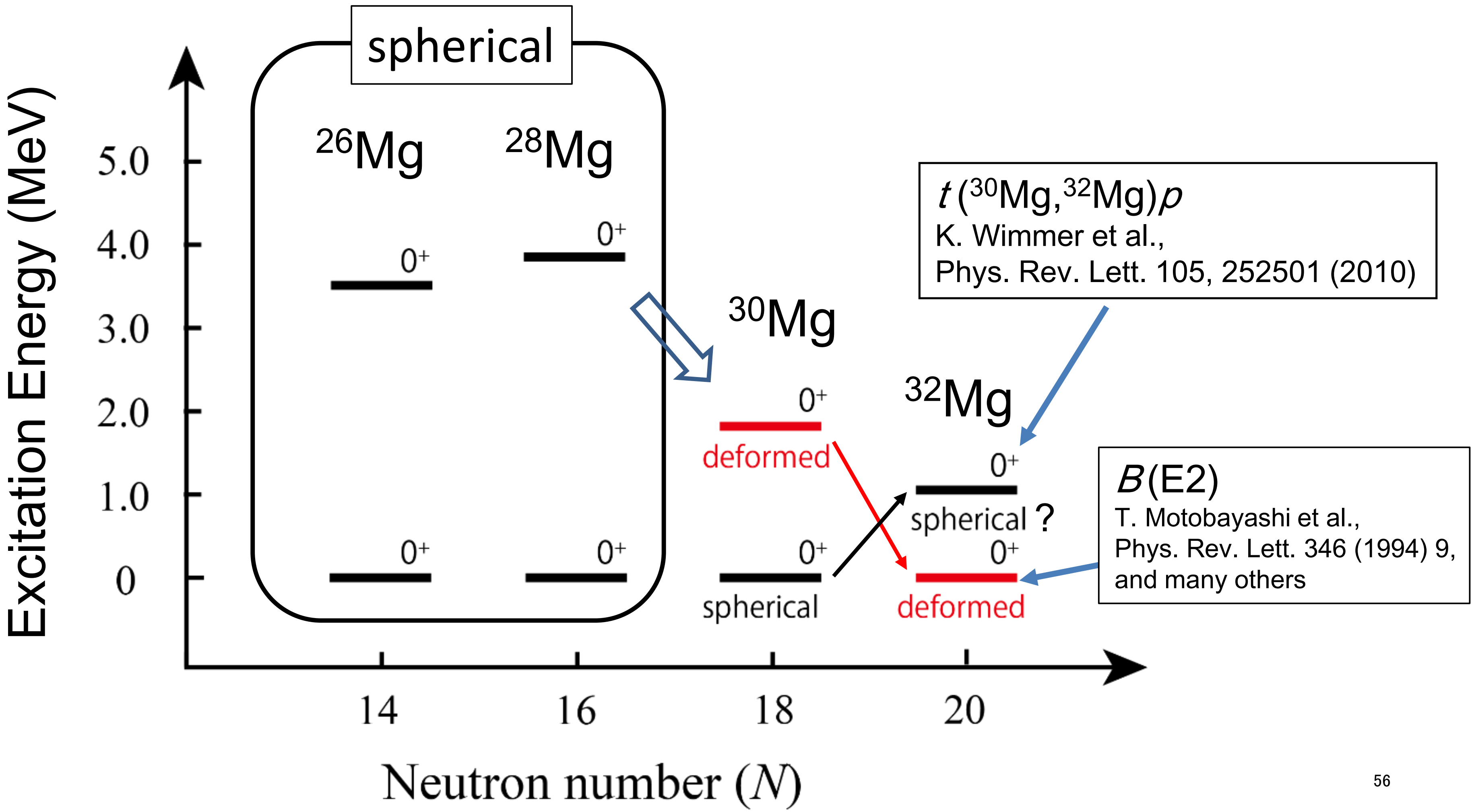

Revised Decay Scheme of ^{28,29}Na and New Levels in ^{28,29}Mg

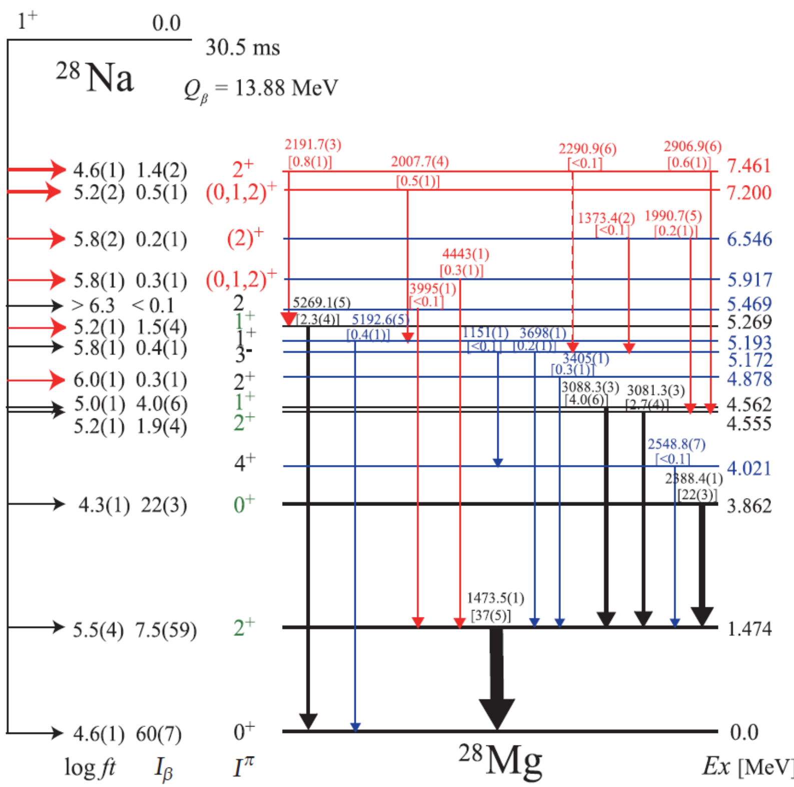

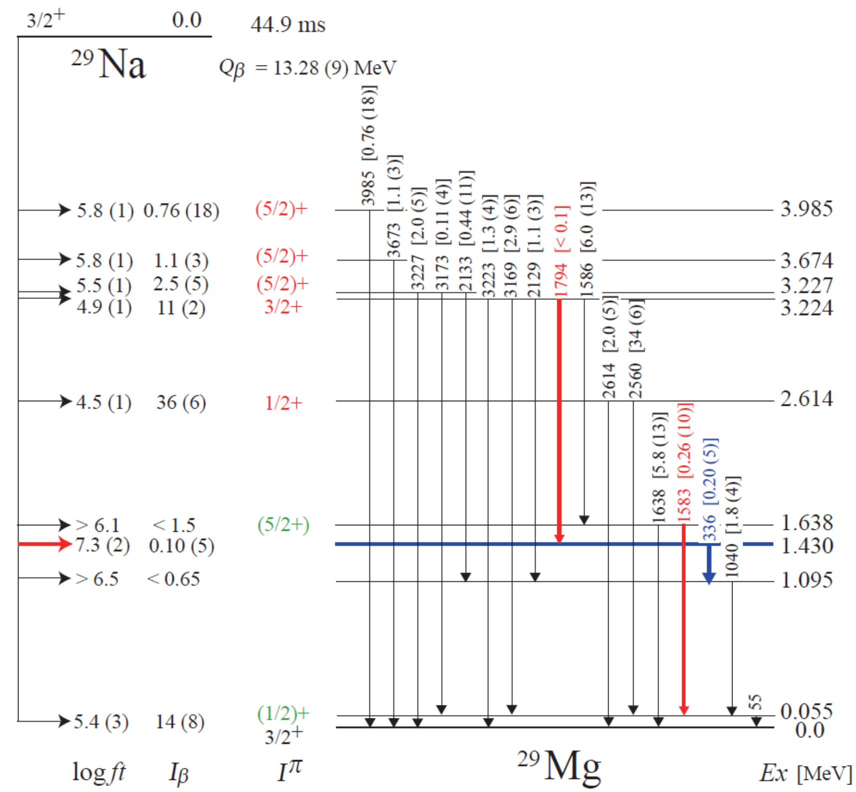

13 γ rays & 9 energy levels
Spins & parities of 4 levels

3 γ rays & 1 energy levels
Spins & parities of 7 levels

Enlargement of the magnetic field by magnet

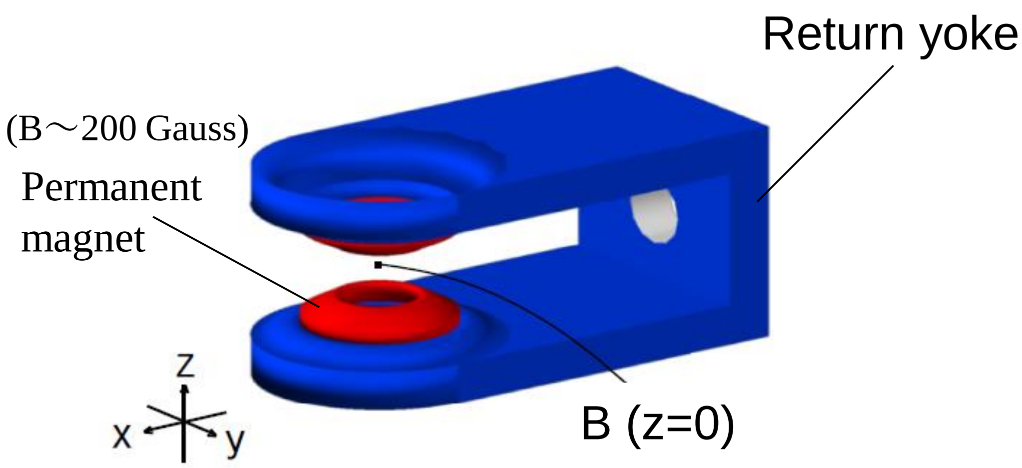

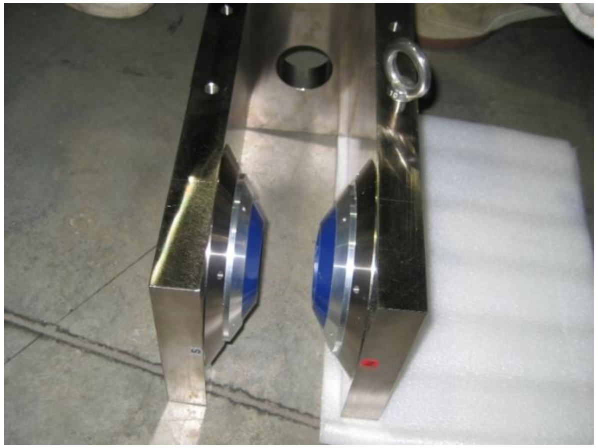

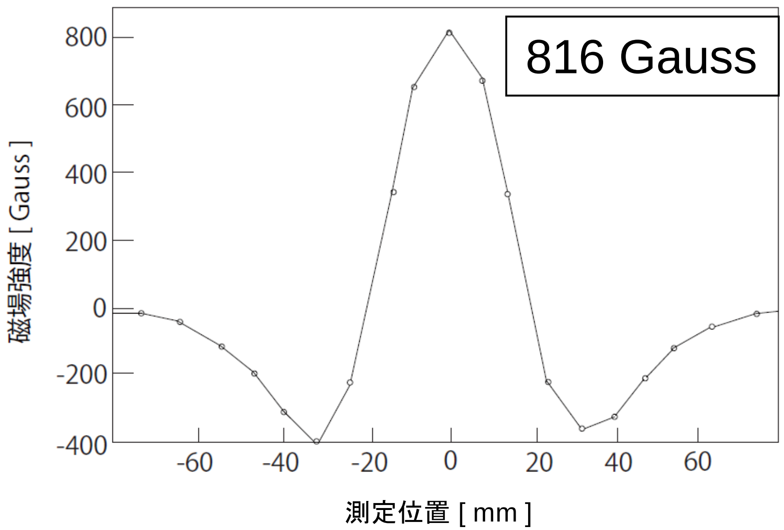

ＴＯＳＣＡ simulation

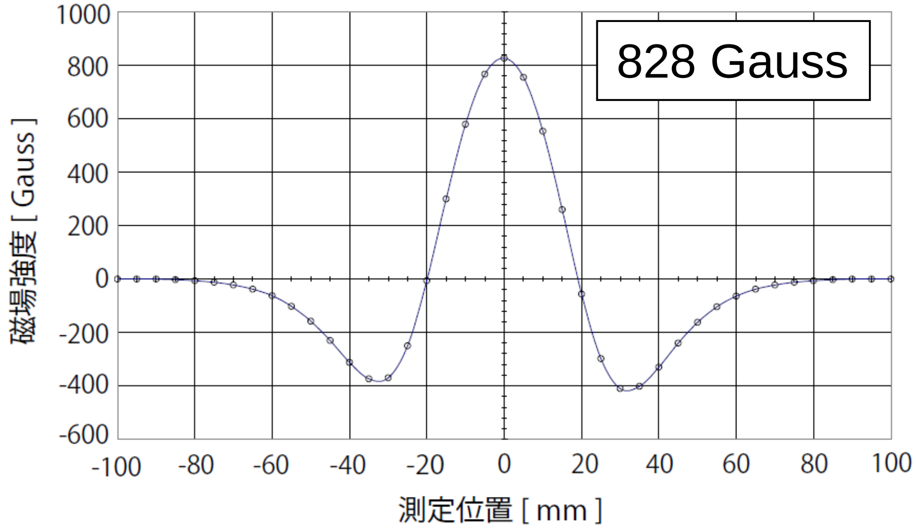

Exp.

static magnet to preserve polarization